Theory of acousto-optic scattering in opaque media in the regime of nonlocal optics

O. Keller
Physics Laboratory, University of Aalborg, Pontoppidanstraede 103, DK-9220 Aalborg Øst, Denmark
(Received 21 March 1983; revised manuscript received 3 November 1983)

A theory of acousto-optic scattering from solid-state plasmas, which, on the basis of the Boltzmann equation, takes into account nonlocal electronic transport effects is established. To emphasize the influence of nonlocal effects on the principles of acousto-optic scattering the treatment is limited to the case where the scattering takes place from a purely transverse bulk sound wave which does not ripple the surface. The coherent inelastic scattering from both the incident and reflected acoustic field is considered. The integro-differential equation for the anti-Stokes field is solved with the assumption that the conduction electrons are scattered specularly from the surface. It is demonstrated that the scattering from a *p*-polarized incident electromagnetic field besides a well-known contribution from the plasmaritonlike part of the incident field is composed of free and forced wave terms arising from the plasmonlike part of the incident field and from branch-cut contributions which are of non-plane-wave character. The scattering from a fully degenerate plasma is considered in the fully nonlocal and almost local regimes. Resonant anti-Stokes scattering is treated and a general condition for resonance in the opaque nonlocal frequency regime is given. A few numerical calculations on Al and *n*-InSb are presented and it is shown that first-order Brillouin scattering via the nonlocal part of the incident light field should enable one to scatter from acoustic phonons far out in the Brillouin zone. The theoretical methods used in the present work are similar to those used in studies of the anomalous skin effect and the photoemission process. These methods almost seem to have been overlooked in light scattering studies. It is shown that the present theory is in agreement with the well-known results of local theories of acousto-optic scattering in opaque media in the appropriate limit.

I. INTRODUCTION

In the wake of the pioneering experimental and theoretical Brillouin-scattering investigations on opaque semiconductors and metals, carried out by Sandercock[1,2] and Bennett *et al.*,[3] an increasing number of papers have been concerned with the inelastic scattering of light from acoustic phonons in opaque media.

A remarkable feature of the Brillouin-scattering spectra is the so-called opacity broadening of the spectral peaks caused by the breakdown of optical-wave-vector conservation normal to the surface, a collapse which leads to coupling of the light to acoustic phonons with a spread of wave vectors and hence of frequencies.[4,5] Another prominent feature which can be explained by taking into account phonon reflection at the sample boundary[6,7] is the observed asymmetry of the line shape of the Brillouin spectra.[1]

A competitive mechanism for inelastic light scattering from opaque media is the scattering from surface ripples generated by acoustoelectrically amplified bulk phonons,[8] by thermally excited transverse and longitudinal bulk waves,[9] or by Rayleigh surface waves produced thermally.[9] The calculated Brillouin spectra from thermally excited surface ripples[10–14] show good agreement with measured spectra on solid[9] and liquid[15] metals.

Recently, detailed investigations based on Green's-function calculations of the power spectra of acoustic vibrations in slabs or semi-infinite media have dealt with the line shapes of Brillouin-scattering spectra in opaque materials having flat surfaces.[16–18] Moreover, rather general theories which take into account the interference between the photoelastic and surface corrugation contributions to the Brillouin scattering have been put forward.[13,19]

An acoustic wave may give rise to a bunching of the conduction electrons in metals and semiconductors through various coupling mechanisms.[20] The bunching in turn can cause inelastic scattering of light.[21] With the main emphasis on acousto-optic diffraction in piezoelectric semiconductors, where also the screened indirect photoelastic effect contributes,[22] the inelastic light scattering by nonthermal free-carrier density fluctuations has been studied both theoretically[23] and experimentally.[24] Also, in thermal Brillouin-scattering investigations in metals the free-carrier contribution has been incorporated.[12,13,15]

It has been pointed out that when the crystal is opaque to the incident and scattered light interference effects among the incoming and diffracted beams seem to be of importance.[25] For x rays the necessity of incorporating interference effects to explain, for instance, the Borrman effect[26] has been known for a long time.[27] To treat interference effects one must use a dynamic theory of inelastic light scattering. On the basis of local[28,29] or nonlocal[30] optical models dynamic light scattering effects have been studied theoretically in a so-called two-wave interference approximation. A review article dealing with inelastic light scattering from opaque crystals has been published recently.[31]

In the present work we focus our attention on some of the new aspects of inelastic light scattering in opaque media that occur by incorporating nonlocal electronic transport properties in the description of the incident and scattered light beams. It is well known that these nonlocal transport effects play an essential role for the understanding of the *linear* plasma-optical properties of metals.[32–37] To keep the discussion at a simple level it is assumed that the scattering takes place from a single transverse acoustic mode polarized in such a way that the surface remains flat when the acoustic wave is reflected from it. Basically and in its method of approach the present work is closely related to other *nonlinear nonlocal* optical studies in solid-state plasmas such as those on light-induced material energy flow,[38,39] second-harmonic generation,[39] and the velocity of stationary energy transport.[40] The results presented in the succeeding sections agree with those obtained on the basis of local theories valid, when the mean free path of the free carriers, essentially in comparison to the wavelength and the penetration depth of the electromagnetic wave in the medium, is negligible. To the present author's knowledge all experimental investigations so far have been done with visible light. However, it is expected that substantial deviations will occur between local Brillouin-scattering theories and experiments if these are done by means of (far-) infrared light in (semiconductors) metals. It is the aim of the present nonlocal theory of acousto-optic scattering to take a first step towards the description of (far-) infrared light scattering in opaque media.

The main body of this paper is organized as follows. With the integro-differential equation of the scattered electromagnetic field as a starting point the general framework of the nonlocal theory of acousto-optic scattering is established in Sec. II. We summarize a nonlocal description of the incident electromagnetic field inside a semi-infinite solid-state plasma. The description is based on the Maxwell equations and the Boltzmann-Vlasov equation in the relaxation-time approximation. By letting the perturbed distribution function relax, not toward thermal equilibrium, but toward equilibrium at the local electron density we keep a *plasmonlike* term in the incident field. This term opens so to speak a new channel of acousto-optic scattering. We proceed by giving the acoustic displacement field associated with pure transverse (T1) incident and reflected sound waves polarized parallel to the surface and perpendicular to the scattering plane. Next, the nonlinear driving polarization is calculated. Finally, the general expression for the scattered electromagnetic field inside and outside the plasma is determined. The method used to calculate the incident and scattered fields resembles that applied in studies of the anomalous skin effect and the photoemission process from metal surfaces.[33–37] For light scattering investigations this kind of approach almost[6] seems to have been overlooked in the literature.

In Sec. III we treat the scattering process in the case where the incident electromagnetic field is p polarized. The structure of the scattered anti-Stokes field, which becomes s polarized, is investigated by contour integration. It is shown that the pole contributions, which give rise to exponentially damped plane-wave components, consist of (i) forced-wave terms originating in the scattering of the *plasmaritonlike* and *plasmonlike* parts of the incident field, and (ii) free-wave terms necessary for the fulfillment of the boundary conditions for the scattered field at the surface. For a fully degenerate plasma the branch-cut contributions which are associated with single-particle excitations show up in the scattered field inside the plasma as *nonexponentially* decaying terms. For the fully degenerate plasma we emphasize a discussion of the scattered field in what we shall call the near-local regime, i.e., the regime where nonlocal effects are incorporated in lowest order.[38,39] The near-local approach is valid for frequencies around the plasma edge. Finally, we consider phase matching and derive a general condition for resonant anti-Stokes scattering in the opaque frequency regime.

In Sec. IV we stress a few qualitative results for acousto-optic scattering via a s-polarized incident field. In Sec. V some quantitative numerical calculations on a metal (Al) and a semiconductor (n-type InSb) are presented. Spectra are shown both as functions of the frequency of light and as functions of the acoustic wave vector. It is demonstrated that the scattering strength via the *plasmonlike* part of the incident field should enable one to pick up acoustic waves far out in the Brillouin zone. Some concluding remarks which concern a comparison with local acousto-optic theories and which point out important limitations of the present approach are made in Sec. VI.

II. FUNDAMENTAL NONLOCAL THEORY

A. Integro-differential equation of the scattered electromagnetic field

Let us consider the *ionic* and *free-carrier* responses of an absorbing crystal to a time and space-varying self-consistent electromagnetic field, and let us assume that the inelastic scattering of light is dominated by scattering from the modulations in the ionic part of the dielectric tensor. The neglect of the free-carrier contribution to the *nonlinear* polarization can be justified for instance in scattering configurations where the contribution from the direct photoelastic effect is polarized perpendicular to the contribution from the bunched free carriers.[23,24,30] In piezoelectric semiconductors such as n-type InSb the use of acoustoelectrically inactive sound waves[20] avoids the bunching of the free carriers and hence their contribution to the nonlinear polarization.

By assuming the free-carrier response to the self-consistent electromagnetic field of the incident light to be *linear* (L) and *nonlocal* in space, and by making use of the time invariance of the material properties of the conduction-electron system, one obtains the following relation between the Fourier transforms in time of the linear free-carrier current density, $\vec{J}^{\,L}(\vec{r},t)$, and the self-consistent electric field, $\vec{E}(\vec{r},t)$,

$$\vec{J}^{\,L}(\vec{r},\omega)=\int_{-\infty}^{\infty}\int_{-\infty}^{\infty}\int_{-\infty}^{\infty}\vec{\vec{\sigma}}^{\,L}(\vec{r},\vec{r}',\omega)\cdot\vec{E}(\vec{r}',\omega)d^3r' , \tag{2.1}$$

where $\vec{\vec{\sigma}}^{\,L}(\vec{r},\vec{r}',\omega)$ is the linear conductivity tensor kernel

at the frequency ω.

For the ionic system we shall adopt a description where the response to the self-consistent field, composed of a *linear* and a *nonlinear* (NL) part giving rise to the inelastic light scattering, is *local* in space. This approach implies that the Fourier transform of the dielectric polarization, $\vec{P}(\vec{r},\omega)$, can be written

$$\vec{P}(\vec{r},\omega)=\epsilon_0\overleftrightarrow{\chi}^{L}(\omega)\cdot\vec{E}(\vec{r},\omega)+\vec{P}^{\,NL}(\vec{r},\omega)\ , \tag{2.2}$$

where $\overleftrightarrow{\chi}^{L}(\omega)$ is the local and linear dielectric susceptibility tensor of the homogeneous medium under study, and $\vec{P}^{\,NL}(\vec{r},\omega)$ is the nonlinear driving polarization, which is the source of the inelastically scattered electromagnetic field.

By means of the Maxwell equations and the constitutive relations in Eqs. (2.1) and (2.2) the time-independent wave equation of the scattered electric field in the kinematic approximation takes the form

$$\{\vec{\nabla}\,\vec{\nabla}-\overleftrightarrow{1}[\nabla^2+(\omega_s/c_0)^2]-(\omega_s/c_0)^2\overleftrightarrow{\chi}^{L}(\omega_s)\}\cdot\vec{E}_s(\vec{r},\omega_s)$$
$$-i\mu_0\omega_s\int_{-\infty}^{\infty}\int_{-\infty}^{\infty}\int_{-\infty}^{\infty}\overleftrightarrow{\sigma}^{L}(\vec{r},\vec{r}\,',\omega_s)\cdot\vec{E}_s(\vec{r}\,',\omega_s)d^3r'=\mu_0\omega_s^2\vec{P}_s^{\,NL}(\vec{r},\omega_s)\ , \tag{2.3}$$

where $\vec{\nabla}$ is the nabla operator, $\overleftrightarrow{1}$ is a unit dyadic of dimension 3×3, c_0 is the velocity of light in vacuum, and μ_0 is the vacuum permeability. Subscript s has been imposed on various quantities in the above integro-differential equation to stress that they belong to the frequency ω_s of the scattered (s) field. In the following, for simplicity, we shall assume that the crystal is isotropic as far as local effects are concerned.

B. Incident electromagnetic field

Let us assume that the solid occupies the half-space $z>0$, the rest of space being vacuum, and let a harmonic electromagnetic wave of angular frequency ω_i, i.e.,

$$\vec{E}_{i0}(\vec{r},t)=\vec{E}_{i0}(k_i^{\parallel},\omega_i)\exp\{i[(\omega_i/c_0)^2-(k_i^{\parallel})^2]^{1/2}z\}$$
$$\times\exp[i(\vec{k}_i^{\,\parallel}\cdot\vec{r}-\omega_i t)] \tag{2.4}$$

be incident on the surface at an oblique angle determined by $\vec{k}_i^{\,\parallel}$, the component of the vacuum wave vector of the electromagnetic field parallel to the surface. For convenience, the plane of incidence is chosen to coincide with the x-z plane of our Cartesian coordinate system. The reflected field outside the crystal is given by

$$\vec{E}_{r0}(\vec{r},t)=\vec{E}_{r0}(k_i^{\parallel},\omega_i)\exp\{-i[(\omega_i/c_0)^2-(k_i^{\parallel})^2]^{1/2}z\}$$
$$\times\exp[i(\vec{k}_i^{\,\parallel}\cdot\vec{r}-\omega_i t)]\ . \tag{2.5}$$

In a recent work[38] the incident electric field inside the solid and the amplitude of the reflected field have been determined by combining the Maxwell equations and the Boltzmann-Vlasov equation in the relaxation-time approximation. In summary, the transmitted field takes the form

$$\vec{E}_i(\vec{r},t)=\frac{1}{2\pi}\exp[i(\vec{k}_i^{\,\parallel}\cdot\vec{r}-\omega_i t)]$$
$$\times\int_{-\infty}^{\infty}\vec{E}_i(k_i^{\parallel},k_i^{\perp},\omega_i)\exp(ik_i^{\perp}z)dk_i^{\perp}\ , \tag{2.6}$$

where the Fourier amplitude $\vec{E}_i(k_i^{\parallel},k_i^{\perp},\omega_i)$ is given by

$$\vec{E}_i(k_i^{\parallel},k_i^{\perp},\omega_i)=\overleftrightarrow{\Xi}(k_i^{\parallel},k_i^{\perp},\omega_i)$$
$$\cdot\begin{bmatrix}t^p(k_i^{\parallel},\omega_i)E_{i0}^p(k_i^{\parallel},\omega_i)\\ t^s(k_i^{\parallel},\omega_i)E_{i0}^s(k_i^{\parallel},\omega_i)\\ 0\end{bmatrix}\ . \tag{2.7}$$

For brevity, we have introduced the second-order tensor

$$\overleftrightarrow{\Xi}(k_i^{\parallel},k_i^{\perp},\omega_i)=2(\{(\omega_i/c_0)^2[1+\chi^L(\omega_i)]-k_i^2\}\overleftrightarrow{1}$$
$$+\vec{k}_i\vec{k}_i+i\mu_0\omega_i\overleftrightarrow{\sigma}^{L}(k_i^{\parallel},k_i^{\perp},\omega_i))^{-1}\ , \tag{2.8}$$

where $\vec{k}_i=\vec{k}_i^{\,\parallel}+k_i^{\perp}\vec{e}_z$, $\vec{e}_z$ being a unit vector in the positive z direction. The Fourier transform $\overleftrightarrow{\sigma}^{L}(k_i^{\parallel},k_i^{\perp},\omega_i)$ of the linear conductivity tensor kernel is obtained from the nonlocal constitutive relation between the free-carrier current density and the self-consistent field. By assuming the conduction electrons to be scattered specularly at the surface, and by assuming the relaxation of the perturbed distribution function of the electrons to be toward equilibrium at the local electron density, the explicit expression for $\overleftrightarrow{\sigma}^{L}(k_i^{\parallel},k_i^{\perp},\omega_i)$ becomes[35,41]

$$\overleftrightarrow{\sigma}^{L}(k_i^{\parallel},k_i^{\perp},\omega_i)=[\overleftrightarrow{1}-\vec{R}(k_i^{\parallel},k_i^{\perp},\omega_i)\vec{k}_i]^{-1}\cdot\overleftrightarrow{\sigma}^{L,s}(k_i^{\parallel},k_i^{\perp},\omega_i)\ , \tag{2.9}$$

where the conductivity tensor kernel $\overleftrightarrow{\sigma}^{L,s}(k_i^{\parallel},k_i^{\perp},\omega_i)$ appropriate to s-polarized mode propagation is given by[38]

$$\overleftrightarrow{\sigma}^{L,s}(k_i^{\parallel},k_i^{\perp},\omega_i)=\frac{e^2\tau}{4\pi^3}\left[\frac{m^*}{\hbar}\right]^3\int_{-\infty}^{\infty}\int_{-\infty}^{\infty}\int_{-\infty}^{\infty}\left[-\frac{\partial f_0(\mathscr{E})}{\partial\mathscr{E}}\right]\frac{\vec{v}\,\vec{v}}{1+i(\vec{k}_i\cdot\vec{v}-\omega_i)\tau}d^3v \tag{2.10}$$

and

$$\vec{R}(k_i^{||},k_i^{\perp},\omega_i)=\frac{1}{4\pi^3\omega_i}\left[\frac{m^*}{\hbar}\right]^3\frac{\partial\mu}{\partial N}\bigg|_{N=N_0}\int_{-\infty}^{\infty}\int_{-\infty}^{\infty}\int_{-\infty}^{\infty}\left[-\frac{\partial f_0(\mathscr{E})}{\partial\mathscr{E}}\right]\frac{\vec{v}}{1+i(\vec{k}_i\cdot\vec{v}-\omega_i)\tau}d^3v\ . \tag{2.11}$$

It should be emphasized that the relaxation of the free-carrier distribution function toward the local electron density allows us to incorporate charge-density fluctuations caused by p-polarized light. This turns out to be essential for the infrared acousto-optic light scattering process discussed in the following as well as for studies of kinetic energy transport associated with p-polarized light-induced free-carrier flows.[41] In Eqs. (2.10) and (2.11), $f_0(\mathscr{E})$ is the Fermi-Dirac distribution function, m^* is the scalar effective mass of the free carriers, and τ, $\mathscr{E}$, $\vec{v}$, and $-e$ are the momentum relaxation time, the kinetic energy, the velocity, and the charge of the free carriers. The derivative of the chemical potential μ with respect to the local electron density N is to be evaluated at the thermal equilibrium electron density N_0.

The normalized field gradients of the incident field at the surface [Eq. (2.7)] are given by[38,39]

$$t^s(k_i^{||},\omega_i)=\frac{4\pi}{\int_{-\infty}^{\infty}\left[1+\frac{k_i^{\perp}}{k_{i0}^{\perp}}\right]\Xi_{yy}(k_i^{||},k_i^{\perp},\omega_i)dk_i^{\perp}} \tag{2.12}$$

and

$$t^p(k_i^{||},\omega_i)=\frac{4\pi}{\int_{-\infty}^{\infty}\left[\left[\frac{c_0k_i^{\perp}}{\omega_i}+\frac{\omega_i}{c_0k_{i0}^{\perp}}\right]\Xi_{xx}(k_i^{||},k_i^{\perp},\omega_i)-\frac{c_0k_i^{||}}{\omega_i}\Xi_{xz}(k_i^{||},k_i^{\perp},\omega_i)\right]dk_i^{\perp}}\ , \tag{2.13}$$

where

$$k_{i0}^{\perp}=[(\omega_i/c_0)^2-(k_i^{||})^2]^{1/2}\ .$$

The amplitudes of the s- and p-polarized incident fields in vacuum have been denoted by E_{i0}^s and E_{i0}^p, respectively.

C. Acoustic displacement field

To emphasize the influence of nonlocal electronic transport effects on the principles of acousto-optic scattering we shall avoid the complications arising from the scattering of light by surface corrugations. Hence we limit ourselves to the most simple case where the inelastic scattering takes place from acoustic displacement field gradients associated with a purely transverse (T1) sound wave polarized parallel to the surface along the y direction. The sound wave will be reflected from the surface of the isotropic medium, and the acousto-optic scattering from both the incident and reflected mode will be considered.

Let the displacement of the incident (i) sound wave be given by

$$\vec{u}_i^{\,T1}(\vec{r},t)=u_i^{T1}(\vec{Q},\Omega)\vec{e}_y\exp[i(\vec{Q}^{||}\cdot\vec{r}-\Omega t)]\exp(-iQ^{\perp}z),\quad Q_{\perp}\geq 0 \tag{2.14}$$

where Ω is the acoustic angular frequency, $u_i^{T1}(\vec{Q},\Omega)$ is the amplitude of the wave, and $\vec{e}_y$ is a unit vector in the positive y direction. By assuming that the lifetime of the mode is infinite and that the damping of the wave in space can be neglected, the frequency Ω and the wave vector $\vec{Q}$ become real quantities. In Eq. (2.14) the wave vector has been split into its components parallel ($||$) and perpendicular ($\perp$) to the surface, i.e., $\vec{Q}=\vec{Q}^{||}-Q^{\perp}\vec{e}_z$, $Q^{\perp}\geq 0$.

Reflection of the sound wave at a stress-free boundary gives total reflection with zero phase angle so that the displacement associated with the reflected (r) mode becomes

$$\vec{u}_r^{\,T1}(\vec{r},t)=u_i^{T1}(\vec{Q},\Omega)\vec{e}_y\exp[i(\vec{Q}^{||}\cdot\vec{r}-\Omega t)]\exp(iQ^{\perp}z)\ , \tag{2.15}$$

remembering that Ω and $\vec{Q}^{||}$ are conserved in the reflection process.

The total displacement field, $\vec{u}^{\,T1}=\vec{u}_i^{\,T1}+\vec{u}_r^{\,T1}$, is of standing-wave character in the z direction, and does not ripple the surface. The acoustic wave vector and frequency are related via an appropriate dispersion relation.

D. Nonlinear driving polarization

When the inelastic scattering of light takes place through the elasto-optic effect the nonlinear driving polarization can be written in the form

$$\vec{P}_s^{\,NL}(\vec{r},\omega_s)=\epsilon_0\overleftrightarrow{\chi}_{si}^{\,NL}(\vec{r},\omega_i,\omega_s,\Omega)\cdot\vec{E}_i(\vec{r},\omega_i)\ , \tag{2.16}$$

where we have introduced a *transition susceptibility* $\overleftrightarrow{\chi}_{si}^{\,NL}$ for transition from the initial state i to the final state s as follows:

$$\overleftrightarrow{\chi}_{si}^{\,NL}(\vec{r},\omega_i,\omega_s,\Omega)=\tfrac{1}{2}\overleftrightarrow{\chi}^{\omega_s,\omega_i,\Omega}:[\vec{\nabla}\vec{u}(\vec{r},\Omega)]\delta(\omega_s-\omega_i-\Omega)+\tfrac{1}{2}\overleftrightarrow{\chi}^{\omega_s,\omega_i,-\Omega}:[\vec{\nabla}\vec{u}(\vec{r},\Omega)]^*\delta(\omega_s-\omega_i+\Omega)\ . \tag{2.17}$$

The quantities $\overleftrightarrow{\chi}^{\omega_s,\omega_i,\Omega}$ and $\overleftrightarrow{\chi}^{\omega_s,\omega_i,-\Omega}$ are the *fourth-order elasto-optic susceptibility tensors* corresponding to anti-Stokes (A) and Stokes (S) scattering processes, respectively. These tensors are discussed in the book by Nelson.[42] The trivial factor of $\frac{1}{2}$ in Eq. (2.17) which does not appear in the treatment of Nelson[42] results from the fact that the Fourier amplitudes of the fields here ($\vec{F}$) are related to those of Nelson ($\vec{F}_N$) by $\vec{F}=2\vec{F}_N$. The space-dependent parts of the acoustic displacement and the incident electric field are denoted by $\vec{u}(\vec{r},\Omega)$ and $\vec{E}_i(\vec{r},\omega_i)$ in Eqs. (2.16) and (2.17) and the Dirac δ function by δ.

In contracted notation the fourth-order elasto-optic susceptibility tensor of an isotropic solid has the form

$$\overleftrightarrow{\chi}^{\omega_s,\omega_i,\pm\Omega}=\begin{bmatrix}\chi_{11} & \chi_{12} & \chi_{12} & 0 & 0 & 0\\ \chi_{12} & \chi_{11} & \chi_{12} & 0 & 0 & 0\\ \chi_{12} & \chi_{12} & \chi_{11} & 0 & 0 & 0\\ 0 & 0 & 0 & \chi_{44} & 0 & 0\\ 0 & 0 & 0 & 0 & \chi_{44} & 0\\ 0 & 0 & 0 & 0 & 0 & \chi_{44}\end{bmatrix}, \tag{2.18}$$

where $\chi_{44}=\frac{1}{2}(\chi_{11}-\chi_{12})$. For brevity we have written $\chi_{ij}^{\omega_s,\omega_i,\pm\Omega}\equiv\chi_{ij}$. When the acoustic displacement field is given by the sum of Eqs. (2.14) and (2.15) one obtains via Eqs. (2.17) and (2.18) the following expression for the transition susceptibility:

$$\begin{aligned}\overleftrightarrow{\chi}_{si}^{\mathrm{NL}}(\vec{r},\omega_i,\omega_s,\Omega)=&\frac{i}{2}\chi_{44}^{\omega_s,\omega_i,\Omega}u_i^{\mathrm{T1}}(\vec{Q},\Omega)\exp(i\vec{Q}^{\,\parallel}\cdot\vec{r})\\ &\times\left[\exp(iQ^{\perp}z)\begin{bmatrix}0 & Q^{\parallel} & 0\\ Q^{\parallel} & 0 & Q^{\perp}\\ 0 & Q^{\perp} & 0\end{bmatrix}+\exp(-iQ^{\perp}z)\begin{bmatrix}0 & Q^{\parallel} & 0\\ Q^{\parallel} & 0 & -Q^{\perp}\\ 0 & -Q^{\perp} & 0\end{bmatrix}\right]\\ &\times\delta(\omega_s-\omega_i-\Omega)-\frac{i}{2}\chi_{44}^{\omega_s,\omega_i,-\Omega}[u_i^{\mathrm{T1}}(\vec{Q},\Omega)]^*\exp(-i\vec{Q}^{\,\parallel}\cdot\vec{r})\\ &\times\left[\exp(-iQ^{\perp}z)\begin{bmatrix}0 & Q^{\parallel} & 0\\ Q^{\parallel} & 0 & Q^{\perp}\\ 0 & Q^{\perp} & 0\end{bmatrix}+\exp(iQ^{\perp}z)\begin{bmatrix}0 & Q^{\parallel} & 0\\ Q^{\parallel} & 0 & -Q^{\perp}\\ 0 & -Q^{\perp} & 0\end{bmatrix}\right]\delta(\omega_s-\omega_i+\Omega)\,.\end{aligned} \tag{2.19}$$

When the incident electromagnetic wave is s polarized the nonlinear driving polarization becomes p polarized and vice versa. By combining Eqs. (2.16) and (2.19) it is a straightforward matter to write the explicit expressions for the nonlinear polarization in these cases.

E. Scattered electromagnetic field

By combining Eqs. (2.6), (2.16), and (2.19), it is realized that the nonlinear driving polarization can be written as follows:

$$\vec{P}_s^{\mathrm{NL}}(\vec{r},\omega_s)=\vec{P}_A^{\mathrm{NL}}(k_A^{\parallel},\omega_A,z)\exp(i\vec{k}_A^{\,\parallel}\cdot\vec{r})\delta(\omega_s-\omega_A)+\vec{P}_S^{\mathrm{NL}}(k_S^{\parallel},\omega_S,z)\exp(i\vec{k}_S^{\,\parallel}\cdot\vec{r})\delta(\omega_s-\omega_S)\,, \tag{2.20}$$

where the x and z dependence have been separated. The explicit expressions for the nonlinear polarizations at the anti-Stokes ($\omega_A=\omega_i+\Omega$) and the Stokes ($\omega_S=\omega_i-\Omega$) frequencies, i.e., $\vec{P}_A^{\mathrm{NL}}(k_A^{\parallel},\omega_A,z)$ and $\vec{P}_S^{\mathrm{NL}}(k_S^{\parallel},\omega_S,z)$, can easily be written by means of Eqs. (2.6) and (2.19). The wave-vector components of the anti-Stokes and Stokes scattered fields parallel to the surface which were introduced in Eq. (2.20) are given by

$$\vec{k}_A^{\,\parallel}=\vec{k}_i^{\,\parallel}+\vec{Q}^{\,\parallel} \tag{2.21}$$

and

$$\vec{k}_S^{\,\parallel}=\vec{k}_i^{\,\parallel}-\vec{Q}^{\,\parallel}\,, \tag{2.22}$$

respectively.

Let us determine now the scattered anti-Stokes field inside, $\vec{E}_A(\vec{r},\omega_A)\exp(-i\omega_A t)$, and outside,

$\vec{E}_{A0}(\vec{r},\omega_A)\exp(-i\omega_A t)$, the solid-state plasma. By making the ansatz

$$\vec{E}_A(\vec{r},\omega_A)=\vec{E}_A(k_A^{\parallel},\omega_A,z)\exp(i\vec{k}_A^{\parallel}\cdot\vec{r}) , \tag{2.23}$$

one obtains, via Eq. (2.3), the following integro-differential equation for the anti-Stokes field:

$$\overleftrightarrow{\mathscr{L}}\left[k_A^{\parallel},\omega_A,\frac{d}{dz},\frac{d^2}{dz^2}\right]\cdot\vec{E}_A(k_A^{\parallel},\omega_A,z)+i\mu_0\omega_A\int_{-\infty}^{\infty}\overleftrightarrow{\sigma}^L(k_A^{\parallel},\omega_A,z-z')\cdot\vec{E}_A(k_A^{\parallel},\omega_A,z')dz'=-\mu_0\omega_A^2\vec{P}_A^{\,\mathrm{NL}}(k_A^{\parallel},\omega_A,z) , \tag{2.24}$$

where the linear tensorial operator $\overleftrightarrow{\mathscr{L}}$ is given by

$$\overleftrightarrow{\mathscr{L}}\left[k_A^{\parallel},\omega_A,\frac{d}{dz},\frac{d^2}{dz^2}\right]=\overleftrightarrow{\mathbb{I}}\left[\frac{d^2}{dz^2}+\left[\frac{\omega_A}{c_0}\right]^2[1+\chi^L(\omega_A)]-(k_A^{\parallel})^2\right]-\vec{O}\vec{O} . \tag{2.25}$$

The vectorial operator $\vec{O}$, introduced for brevity, has the form

$$\vec{O}\left[k_A^{\parallel},\frac{d}{dz}\right]=i\vec{k}_A^{\parallel}+\vec{e}_z\frac{d}{dz} . \tag{2.26}$$

In deriving Eq. (2.24) we have made use of the redefinition of the electric field $E_{A,x}(k_A^{\parallel},\omega_A,z)=E_{A,x}(k_A^{\parallel},\omega_A,-z)$, $E_{A,y}(k_A^{\parallel},\omega_A,z)=E_{A,y}(k_A^{\parallel},\omega_A,-z)$, and $E_{A,z}(k_A^{\parallel},\omega_A,z)=-E_{A,z}(k_A^{\parallel},\omega_A,-z)$ for $z<0$, and introduced the Fourier amplitude $\overleftrightarrow{\sigma}^L(k_A^{\parallel},\omega_A,z-z')$ corresponding to Fourier integral transformations of the conductivity tensor kernel in the coordinates $x-x'$ and $y-y'$ parallel to the surface.

The final step in the determination of the scattered anti-Stokes field is taken by inserting the Fourier integral transformations

$$\vec{E}_A(k_A^{\parallel},\omega_A,z)=\frac{1}{2\pi}\int_{-\infty}^{\infty}\vec{E}_A(k_A^{\parallel},k_A^{\perp},\omega_A)\exp(ik_A^{\perp}z)dk_A^{\perp} \tag{2.27}$$

and

$$\vec{P}_A^{\,\mathrm{NL}}(k_A^{\parallel},\omega_A,z)=\frac{1}{2\pi}\int_{-\infty}^{\infty}\vec{P}_A^{\,\mathrm{NL}}(k_A^{\parallel},k_A^{\perp},\omega_A)\times\exp(ik_A^{\perp}z)dk_A^{\perp} \tag{2.28}$$

into Eq. (2.24), and using a technique identical to that described in Ref. 38. Hence one obtains

$$\vec{E}_A(k_A^{\parallel},k_A^{\perp},\omega_A)=\overleftrightarrow{\Xi}(k_A^{\parallel},k_A^{\perp},\omega_A)\cdot\left[\vec{g}(k_A^{\parallel},\omega_A,z\to0^+)-\frac{\mu_0}{2}\omega_A^2\vec{P}_A^{\,\mathrm{NL}}(k_A^{\parallel},k_A^{\perp},\omega_A)\right] , \tag{2.29}$$

where the second-order tensor $\overleftrightarrow{\Xi}$ is given by Eq. (2.8) with the replacements $k_i^{\parallel},k_i^{\perp},\omega_i\to k_A^{\parallel},k_A^{\perp},\omega_A$. The vector $\vec{g}$ consists of appropriate field derivatives of the anti-Stokes field at the surface, i.e.,

$$\vec{g}(k_A^{\parallel},\omega_A,z\to0^+)=\begin{bmatrix}\dfrac{\partial E_{A,x}(k_A^{\parallel},\omega_A,z\to0^+)}{\partial z}\\ \dfrac{\partial E_{A,y}(k_A^{\parallel},\omega_A,z\to0^+)}{\partial z}\\ 0\end{bmatrix} . \tag{2.30}$$

The scattered anti-Stokes field $\vec{E}_{A0}(\vec{r},t)$ *outside* the crystal can be expressed as follows:

$$\vec{E}_{A0}(\vec{r},t)=\vec{E}_{A0}(k_A^{\parallel},\omega_A)\times\exp\{-i[(\omega_A/c_0)^2-(k_A^{\parallel})^2]^{1/2}z\}\times\exp[i(\vec{k}_A^{\parallel}\cdot\vec{r}-\omega_A t)] . \tag{2.31}$$

In principle, the scattered anti-Stokes field inside and outside the solid-state plasma now is completely determined if the field derivatives $g_x(k_A^{\parallel},\omega_A,z\to0^+)$ and $g_y(k_A^{\parallel},\omega_A,z\to0^+)$ at the surface and the field amplitude $\vec{E}_{A0}(k_A^{\parallel},\omega_A)$ are known. These quantities are determined by means of the boundary conditions for the electric and magnetic fields at the sharp, nonmoving boundary. Since $\overleftrightarrow{\Xi}$ has the general form [see Eq. (2.8)]

$$\overleftrightarrow{\Xi}=\begin{bmatrix}\Xi_{xx}&0&\Xi_{xz}\\0&\Xi_{yy}&0\\\Xi_{zx}&0&\Xi_{zz}\end{bmatrix} , \tag{2.32}$$

and the acoustic wave vector $\vec{Q}$ is parallel to the xz plane, the cases where s- and p-polarized modes are incident upon the crystal can be treated separately. Note that $\overleftrightarrow{\Xi}$ is symmetric, i.e., $\Xi_{xz}=\Xi_{zx}$. In the next two sections we shall consider the uncoupled s- and p-scattering configurations in turn. The results derived in this section for the anti-Stokes field does of course hold for the Stokes field if one makes the replacement $A\to S$, i.e., essentially $\vec{k}_A^{\parallel}\to\vec{k}_S^{\parallel}$ and $\omega_A\to\omega_S$.

III. SCATTERING OF A p-POLARIZED INCIDENT FIELD

A. General results

Let us consider the case where the incident electromagnetic wave is p polarized. By combining Eqs. (2.6), (2.7), (2.16), (2.19), and (2.32) one obtains the following expression for the s-polarized driving polarization at the anti-Stokes frequency:

$$\vec{P}_A^{\mathrm{NL},s}(k_A^{\parallel},\omega_A,z)=\frac{i}{4\pi}\epsilon_0 u_i^{\mathrm{T1}}(\vec{Q},\Omega)t^p(k_i^{\parallel},\omega_i)E_{i0}^p(k_i^{\parallel},\omega_i)\chi_{44}^{\omega_A,\omega_i,\Omega}\vec{e}_y$$
$$\times\left[Q^{\parallel}[\exp(iQ^{\perp}z)+\exp(-iQ^{\perp}z)]\int_{-\infty}^{\infty}\Xi_{xx}(k_i^{\parallel},k_i^{\perp},\omega_i)\exp(ik_i^{\perp}z)dk_i^{\perp}\right.$$
$$\left.+Q^{\perp}[\exp(iQ^{\perp}z)-\exp(-iQ^{\perp}z)]\int_{-\infty}^{\infty}\Xi_{xz}(k_i^{\parallel},k_i^{\perp},\omega_i)\exp(ik_i^{\perp}z)dk_i^{\perp}\right]. \tag{3.1}$$

With the redefinition

$$P_A^{\mathrm{NL},s}(k_A^{\parallel},\omega_A,z)\vec{e}_y=P_A^{\mathrm{NL},s}(k_A^{\parallel},\omega_A,-z)\vec{e}_y \quad \text{for } z<0\ ,$$

the Fourier amplitude $P_A^{\mathrm{NL},s}(k_A^{\parallel},k_A^{\perp},\omega_A)$ of the nonlinear driving polarization is obtained by inserting Eq. (3.1) into the inverse of Eq. (2.28), interchanging the order of integration, and using the δ function expansion

$$\delta(x)=(2\pi)^{-1}\int_{-in}^{in}\exp(ikx)dk\ .$$

Doing this, one gets

$$\vec{P}_A^{\mathrm{NL},s}(k_A^{\parallel},k_A^{\perp},\omega_A)=\frac{i}{2}\epsilon_0 u_i^{\mathrm{T1}}(\vec{Q},\Omega)t^p(k_i^{\parallel},\omega_i)E_{i0}^p(k_i^{\parallel},\omega_i)\chi_{44}^{\omega_A,\omega_i,\Omega}\vec{e}_y\{Q^{\parallel}[\Xi_{xx}(k_i^{\parallel},k_A^{\perp}-Q^{\perp},\omega_i)+\Xi_{xx}(k_i^{\parallel},k_A^{\perp}+Q^{\perp},\omega_i)]$$
$$+Q^{\perp}[\Xi_{xz}(k_i^{\parallel},k_A^{\perp}-Q^{\perp},\omega_i)-\Xi_{xz}(k_i^{\parallel},k_A^{\perp}+Q^{\perp},\omega_i)]\}. \tag{3.2}$$

Continuity of the tangential component of the anti-Stokes scattered electric and magnetic fields at the surface gives by means of Eqs. (2.27), (2.29), (2.31), and (2.32) two linear equations among the yet unknown quantities g_y and E_{A0}^s. Solving these one obtains

$$g_y(k_A^{\parallel},\omega_A,\ z\to 0^+)=\frac{\mu_0}{8\pi}\omega_A^2 t^s(k_A^{\parallel},\omega_A)\int_{-\infty}^{\infty}\left[1+\frac{k_A^{\perp}}{k_{A0}^{\perp}}\right]\Xi_{yy}(k_A^{\parallel},k_A^{\perp},\omega_A)P_A^{\mathrm{NL},s}(k_A^{\parallel},k_A^{\perp},\omega_A)dk_A^{\perp}\ , \tag{3.3}$$

and

$$E_{A0}^s(k_A^{\parallel},\omega_A)=\frac{\mu_0}{(4\pi)^2}\omega_A^2 t^s(k_A^{\parallel},\omega_A)$$
$$\times\left[\left[\int_{-\infty}^{\infty}\frac{k_A^{\perp}}{k_{A0}^{\perp}}\Xi_{yy}(k_A^{\parallel},k_A^{\perp},\omega_A)P_A^{\mathrm{NL},s}(k_A^{\parallel},k_A^{\perp},\omega_A)dk_A^{\perp}\right]\left[\int_{-\infty}^{\infty}\Xi_{yy}(k_A^{\parallel},k_A^{\perp},\omega_A)dk_A^{\perp}\right]\right.$$
$$\left.-\left[\int_{-\infty}^{\infty}\Xi_{yy}(k_A^{\parallel},k_A^{\perp},\omega_A)P_A^{\mathrm{NL},s}(k_A^{\parallel},k_A^{\perp},\omega_A)dk_A^{\perp}\right]\left[\int_{-\infty}^{\infty}\frac{k_A^{\perp}}{k_{A0}^{\perp}}\Xi_{yy}(k_A^{\parallel},k_A^{\perp},\omega_A)dk_A^{\perp}\right]\right], \tag{3.4}$$

where $k_{A0}^{\perp}=[(\omega_A/c_0)^2-(k_A^{\parallel})^2]^{1/2}$ is the component of the vacuum wave vector of the anti-Stokes scattered field perpendicular to the surface, and where $t^s(k_A^{\parallel},\omega_A)$ is given by Eq. (2.12) if one makes the replacements $k_i^{\parallel},k_i^{\perp},\omega_i\to k_A^{\parallel},k_A^{\perp},\omega_A$.

Outside the crystal the field will be given by Eq. (2.31) with

$$\vec{E}_{A0}(k_A^{\parallel},\omega_A)=E_{A0}^s(k_A^{\parallel},\omega_A)\vec{e}_y\ ,$$

where E_{A0}^s is taken from Eqs. (3.4). Inside the crystal the field takes the form

$$\vec{E}_A^s(\vec{r},t)=\frac{1}{2\pi}\exp[i(\vec{k}_A^{\parallel}\cdot\vec{r}-\omega_A t)]\vec{e}_y$$
$$\times\int_{-\infty}^{\infty}\Xi_{yy}(k_A^{\parallel},k_A^{\perp},\omega_A)\left[g_y(k_A^{\parallel},\omega_A,z\to 0^+)-\frac{\mu_0}{2}\omega_A^2 P_A^{\mathrm{NL},s}(k_A^{\parallel},k_A^{\perp},\omega_A)\right]\exp(ik_A^{\perp}z)dk_A^{\perp}\ , \tag{3.5}$$

where g_y and $P_A^{\mathrm{NL},s}$ are now known.

Immediately, it appears from Eq. (2.19) that the expression for the scattered anti-Stokes field derived in this section can be used for the scattered Stokes field if, in Eq. (3.2) for the Fourier amplitude of the nonlinear driving polarization, one makes the replacements $u_i^{\mathrm{T}1}(\vec{Q},\Omega)\rightarrow[u_i^{\mathrm{T}1}(\vec{Q},\Omega)]^*$, $Q^{\parallel}\rightarrow -Q^{\parallel}$, and $\chi_{44}^{\omega_A,\omega_i,\Omega}\rightarrow\chi_{44}^{\omega_S,\omega_i,-\Omega}$, and besides that, in all relevant equations make the substitution $A\rightarrow S$.

B. Pole contributions

The structure of the scattered anti-Stokes field inside the crystal [Eq. (3.5)] can be investigated more closely by deforming the path of integration along the real axis into an appropriate path in the complex $k_A^{\perp}$ plane. Thus by contour integration in the upper (or lower) part of the complex $k_A^{\perp}$ plane one picks up contributions from branch cuts and poles of the integrand in Eq. (3.5). The pole contributions, corresponding to exponentially decaying plane-wave modes, will be examined in this section.

Let us consider the linear conductivity tensor $\overleftrightarrow{\sigma}^L(k^{\parallel},k^{\perp},\omega)$ given in Eqs. (2.9)–(2.11), omitting for simplicity any subscripts on the wave vector and the frequency. Since the conductivity tensor for specular electron scattering is identical to that of an infinite medium,[33,34,38] and since $\vec{k}$ in Eq. (2.9) is a *real* quantity, the conductivity tensor will be diagonal in a coordinate system which is obtained by a rotation of the original one about the y axis. The angle of rotation must be such that the z axis is brought to coincide with the direction of $\vec{k}$. Thus in the rotated coordinate system (x',y',z') the diagonal elements of the conductivity tensor become $\sigma_{x'x'}^L=\sigma_{y'y'}^L=\sigma_{\mathrm{T}}^L(k,\omega)$ and $\sigma_{z'z'}^L=\sigma_{\mathrm{L}}^L(k,\omega)$, where σ_{T}^L and σ_{L}^L are the transverse and longitudinal linear conductivity response functions of an infinite medium, respectively. The explicit expressions for these response functions need not be specified in this section. The relations between the conductivity tensor elements in the original and rotated coordinate systems are

$$\sigma_{xx}^L(k^{\parallel},k^{\perp},\omega)=(k^{\perp}/k)^2\sigma_{\mathrm{T}}^L(k,\omega)+(k^{\parallel}/k)^2\sigma_{\mathrm{L}}^L(k,\omega)\ , \tag{3.6}$$

$$\sigma_{yy}^L(k^{\parallel},k^{\perp},\omega)=\sigma_{\mathrm{T}}^L(k,\omega)\ , \tag{3.7}$$

$$\sigma_{zz}^L(k^{\parallel},k^{\perp},\omega)=(k^{\parallel}/k)^2\sigma_{\mathrm{T}}^L(k,\omega)+(k^{\perp}/k)^2\sigma_{\mathrm{L}}^L(k,\omega)\ , \tag{3.8}$$

and

$$\sigma_{xz}^L(k^{\parallel},k^{\perp},\omega)=\sigma_{zx}^L(k^{\parallel},k^{\perp},\omega)=\frac{k^{\parallel}k^{\perp}}{k^2}[\sigma_{\mathrm{L}}^L(k,\omega)-\sigma_{\mathrm{T}}^L(k,\omega)]\ , \tag{3.9}$$

where $k^2=(k^{\parallel})^2+(k^{\perp})^2$. The remaining components are equal to zero.

To determine the pole contributions to the scattered anti-Stokes field one must determine Ξ_{xx}, Ξ_{yy}, and Ξ_{xz} explicitly.

By means of Eqs. (2.8), (3.6), (3.8), and (3.9) it appears that

$$\Xi_{xx}(k^{\parallel},k^{\perp},\omega)=\frac{2}{k^2}\left[\frac{(k^{\parallel})^2}{N_{\mathrm{L}}(k,\omega)}+\frac{(k^{\perp})^2}{N_{\mathrm{T}}(k,\omega)}\right] \tag{3.10}$$

and

$$\Xi_{xz}(k^{\parallel},k^{\perp},\omega)=\frac{2k^{\parallel}k^{\perp}}{k^2}\left[\frac{1}{N_{\mathrm{L}}(k,\omega)}-\frac{1}{N_{\mathrm{T}}(k,\omega)}\right]\ , \tag{3.11}$$

where

$$N_{\mathrm{T}}(k,\omega)=(\omega/c_0)^2[1+\chi^L(\omega)]+i\mu_0\omega\sigma_{\mathrm{T}}^L(k,\omega)-k^2 \tag{3.12}$$

and

$$N_{\mathrm{L}}(k,\omega)=(\omega/c_0)^2[1+\chi^L(\omega)]+i\mu_0\omega\sigma_{\mathrm{L}}^L(k,\omega)\ . \tag{3.13}$$

By combining Eqs. (2.8) and (3.7) one gets

$$\Xi_{yy}(k^{\parallel},k^{\perp},\omega)=\frac{2}{N_{\mathrm{T}}(k,\omega)}\ . \tag{3.14}$$

The zeros of the denominators in Eqs. (3.10), (3.11), and (3.14) are determined by the dispersion relations for transverse (T) and longitudinal (L) polarized waves propagating in an unbounded medium, i.e.,

$$N_{\mathrm{T}}(k^{\parallel},\kappa_{\mathrm{T}}^{\perp,n},\omega)=0 \tag{3.15}$$

and

$$N_{\mathrm{L}}(k^{\parallel},\kappa_{\mathrm{L}}^{\perp,n},\omega)=0\ , \tag{3.16}$$

respectively. In Eqs. (3.15) and (3.16) we have split the wave vector into its components parallel and perpendicular to the surface to stress the fact that the wave-vector component parallel to the surface is a *given* real quantity in the present context (essentially $k_i^{\parallel}$ or $k_A^{\parallel}$). The unknown complex wave-vector components perpendicular to the surface, denoted by $\kappa_{\mathrm{T}}^{\perp,n}$ and $\kappa_{\mathrm{L}}^{\perp,n}$, which are to be determined by the above equations, have been given superscript n to indicate that more than one solution eventually exists to Eqs. (3.15) and (3.16) in the nonlocal regime. Thus $n=1,2,\ldots,$ denotes the various solutions. Throughout the paper zeros in the upper (or lower) half-plane of the complex plane only are to be considered. In the following we shall denote the complex wave-vector components perpendicular to the surface which are obtained by solving Eqs. (3.15) and (3.16) for $(k^{\parallel},\omega)=(k_i^{\parallel},\omega_i)$ and $(k_A^{\parallel},\omega_A)$ by $\kappa_{\mathrm{T},i}^{\perp,n}$, $\kappa_{\mathrm{L},i}^{\perp,n}$, $\kappa_{\mathrm{T},A}^{\perp,n}$, and $\kappa_{\mathrm{L},A}^{\perp,n}$, respectively. With this notation the zeros of the "displaced" dispersion relations

$$N_{\mathrm{T}}(k_i^{\parallel},k_A^{\perp}\mp Q^{\perp},\omega_i)=0 \tag{3.17}$$

and

$$N_{\mathrm{L}}(k_i^{\parallel},k_A^{\perp}\mp Q^{\perp},\omega_i)=0 \tag{3.18}$$

are given by

$$k_A^{\perp}=\kappa_{\mathrm{T},i}^{\perp,n}\pm Q^{\perp} \tag{3.19}$$

and

$$k_A^{\perp}=\kappa_{\mathrm{L},i}^{\perp,n}\pm Q^{\perp}\ . \tag{3.20}$$

Now we are prepared to take the last step in the derivation of the pole contributions to the scattered anti-Stokes field. By means of Eqs. (3.10), (3.11), and (3.14) the nonlinear driving polarization in Eq. (3.2) can be written in the form

$$\vec{P}_A^{\mathrm{NL},s}(k_A^{\parallel},k_A^{\perp},\omega_A)=i\epsilon_0 u_i^{\mathrm{T}1}(\vec{Q},\Omega)t^p(k_i^{\parallel},\omega_i)E_{i0}^p(k_i^{\parallel},\omega_i)\chi_{44}^{\omega_A,\omega_i,\Omega}\vec{e}_y \times\sum_{-,+}[(k_i^{\parallel})^2+(k_A^{\perp}\mp Q^{\perp})^2]^{-1}\left[\frac{k_i^{\parallel}[Q^{\parallel}k_i^{\parallel}+Q^{\perp}(k_A^{\perp}\mp Q^{\perp})]}{N_{\mathrm{L}}(k_i^{\parallel},k_A^{\perp}\mp Q^{\perp},\omega_i)}+\frac{(k_A^{\perp}\mp Q^{\perp})[Q^{\parallel}(k_A^{\perp}\mp Q^{\perp})-Q^{\perp}k_i^{\parallel}]}{N_{\mathrm{T}}(k_i^{\parallel},k_A^{\perp}\mp Q^{\perp},\omega_i)}\right]. \tag{3.21}$$

Finally, by combining Eqs. (3.5) and (3.14)—(3.21) and by performing a contour integration along an expanding semicircle in the upper half of the complex $k_A^{\perp}$ plane one obtains the following expression for the scattered anti-Stokes field inside the absorbing solid:

$$\vec{E}_A^s(\vec{r},t)=\vec{e}_y\exp[i(\vec{k}_A^{\parallel}\cdot\vec{r}-\omega_A t)]\sum_{+,-}\sum_n\{a_{\pm}^n\exp(i\kappa_{\mathrm{T},A}^{\perp,n}z)+b_{\mathrm{T},\pm}^n\exp[i(\kappa_{\mathrm{T},i}^{\perp,n}\pm Q^{\perp})z]+b_{\mathrm{L},\pm}^n\exp[i(\kappa_{\mathrm{L},i}^{\perp,n}\pm Q^{\perp})z]\}+\cdots, \tag{3.22}$$

where the ellipsis includes unspecified branch-cut contributions and

$$a_{\pm}^n=\mathscr{R}_{\mathrm{T}}^n(k_A^{\parallel},\kappa_{\mathrm{T},A}^{\perp,n},\omega_A)\left[2ig_y(k_A^{\parallel},\omega_A,z\to0^+)+(\omega_A/c_0)^2\frac{u_i^{\mathrm{T}1}(\vec{Q},\Omega)t^p(k_i^{\parallel},\omega_i)E_{i0}^p(k_i^{\parallel},\omega_i)\chi_{44}^{\omega_A,\omega_i,\Omega}}{(k_i^{\parallel})^2+(\kappa_{\mathrm{T},A}^{\perp,n}\mp Q^{\perp})^2}\times\left[\frac{(\kappa_{\mathrm{T},A}^{\perp,n}\mp Q^{\perp})[Q^{\parallel}(\kappa_{\mathrm{T},A}^{\perp,n}\mp Q^{\perp})-Q^{\perp}k_i^{\parallel}]}{N_{\mathrm{T}}(k_i^{\parallel},\kappa_{\mathrm{T},A}^{\perp,n}\mp Q^{\perp},\omega_i)}+\frac{k_i^{\parallel}[Q^{\parallel}k_i^{\parallel}+Q^{\perp}(\kappa_{\mathrm{T},A}^{\perp,n}\mp Q^{\perp})]}{N_{\mathrm{L}}(k_i^{\parallel},\kappa_{\mathrm{T},A}^{\perp,n}\mp Q^{\perp},\omega_i)}\right]\right], \tag{3.23}$$

$$b_{\mathrm{T},\pm}^n=(\omega_A/c_0)^2u_i^{\mathrm{T}1}(\vec{Q},\Omega)t^p(k_i^{\parallel},\omega_i)E_{i0}^p(k_i^{\parallel},\omega_i)\chi_{44}^{\omega_A,\omega_i,\Omega}\frac{\kappa_{\mathrm{T},i}^{\perp,n}(Q^{\parallel}\kappa_{\mathrm{T},i}^{\perp,n}-Q^{\perp}k_i^{\parallel})}{(k_i^{\parallel})^2+(\kappa_{\mathrm{T},i}^{\perp,n})^2}\frac{\mathscr{R}_T^n(k_i^{\parallel},\kappa_{\mathrm{T},i}^{\perp,n},\omega_i)}{N_{\mathrm{T}}(k_A^{\parallel},\kappa_{\mathrm{T},i}^{\perp,n}\pm Q^{\perp},\omega_A)}, \tag{3.24}$$

and

$$b_{\mathrm{L},\pm}^n=(\omega_A/c_0)^2u_i^{\mathrm{T}1}(\vec{Q},\Omega)t^p(k_i^{\parallel},\omega_i)E_{i0}^p(k_i^{\parallel},\omega_i)\chi_{44}^{\omega_A,\omega_i,\Omega}\frac{k_i^{\parallel}(Q^{\parallel}k_i^{\parallel}+Q^{\perp}\kappa_{\mathrm{L},i}^{\perp,n})}{(k_i^{\parallel})^2+(\kappa_{\mathrm{L},i}^{\perp,n})^2}\frac{\mathscr{R}_L^n(k_i^{\parallel},\kappa_{\mathrm{L},i}^{\perp,n},\omega_i)}{N_{\mathrm{T}}(k_A^{\parallel},\kappa_{\mathrm{L},i}^{\perp,n}\pm Q^{\perp},\omega_A)}. \tag{3.25}$$

By means of Eq. (3.3) the field derivative at the surface $g_y(k_A^{\parallel},\omega_A,z\to0^+)$, appearing in Eq. (3.23), becomes

$$g_y(k_A^{\parallel},\omega_A,z\to0^+)=-\tfrac{1}{2}t^s(k_A^{\parallel},\omega_A)\sum_{+,-}\sum_n\left[\left[1+\frac{\kappa_{\mathrm{T},i}^{\perp,n}\pm Q^{\perp}}{k_{A0}^{\perp}}\right]b_{\mathrm{T},\pm}^n+\left[1+\frac{\kappa_{\mathrm{L},i}^{\perp,n}\pm Q^{\perp}}{k_{A0}^{\perp}}\right]b_{\mathrm{L},\pm}^n+\left[1+\frac{\kappa_{\mathrm{T},A}^{\perp,n}}{k_{A0}^{\perp}}\right]c_{\pm}^b\right]+\cdots, \tag{3.26}$$

where the ellipsis includes unspecified branch-cut contributions and

$$c_{\pm}^n=\left[\frac{\omega_A}{c_0}\right]^2\frac{u_i^{\mathrm{T}1}(\vec{Q},\Omega)t^p(k_i^{\parallel},\omega_i)E_{i0}^p(k_i^{\parallel},\omega_i)\chi_{44}^{\omega_A,\omega_i,\Omega}}{(k_i^{\parallel})^2+(\kappa_{\mathrm{T},A}^{\perp,n}\mp Q^{\perp})^2}\mathscr{R}_{\mathrm{T}}^n(k_A^{\parallel},\kappa_{\mathrm{T},A}^{\perp,n},\omega_A)\times\left[\frac{k_i^{\parallel}[Q^{\parallel}k_i^{\parallel}+Q^{\perp}(\kappa_{\mathrm{T},A}^{\perp,n}\mp Q^{\perp})]}{N_{\mathrm{L}}(k_i^{\parallel},\kappa_{\mathrm{T},A}^{\perp,n}\mp Q^{\perp},\omega_i)}+\frac{(\kappa_{\mathrm{T},A}^{\perp,n}\mp Q^{\perp})[Q^{\parallel}(\kappa_{\mathrm{T},A}^{\perp,n}\mp Q^{\perp})-Q^{\perp}k_i^{\parallel}]}{N_{\mathrm{T}}(k_i^{\parallel},\kappa_{\mathrm{T},A}^{\perp,n}\mp Q^{\perp},\omega_i)}\right] \tag{3.27}$$

and

$$t^s(k_A^{\parallel},\omega_A)=\left[\sum_n i\left[1+\frac{\kappa_{\mathrm{T},A}^{\perp,n}}{k_{A0}^{\perp}}\right]\mathscr{R}_{\mathrm{T}}^n(k_A^{\parallel},\kappa_{\mathrm{T},A}^{\perp,n},\omega_A)+\cdots\right]^{-1}, \tag{3.28}$$

where the ellipsis includes unspecified branch-cut contributions. In deriving Eqs. (3.22)—(3.28) we have assumed simple first-order poles of the integrand in Eq. (3.5), and, for brevity, introduced

$$\mathscr{R}(k^{\parallel},\kappa^{\perp},\omega)=\lim_{k^{\perp}\to\kappa^{\perp}}\left[\frac{k^{\perp}-\kappa^{\perp}}{N(k^{\parallel},k^{\perp},\omega)}\right], \tag{3.29}$$

with the appropriate subscripts and superscripts on $\mathscr{R}$, N, $k^{\parallel}$, $\kappa^{\perp}$, and ω.

The branch-cut contributions to the scattered field normally disappear rather rapidly for large z.[41] Hence, the sum of the exponentially decaying inhomogeneous plane waves in Eq. (3.22) represents the asymptotic solution to the scattered anti-Stokes field. Furthermore, the analysis of the asymptotic behavior often is facilitated by the fact that merely a single solution exists to each of the dispersion relations [Eqs. (3.15) and (3.16)]. Omitting for convenience the index n, the asymptotic solution is composed of (i) one *free-wave* contribution $(a_+ + a_-)\exp(i\kappa_{\mathrm{T},A}^{\perp}z)$, which is necessary for the fulfillment of the boundary conditions of the scattered field at the surface, (ii) two *forced-wave* terms $b_{\mathrm{T},\pm}\exp[i(\kappa_{\mathrm{T},i}^{\perp}\pm Q^{\perp})z]$, arising as a result of the *plasmaritonlike*[43] (or solenoidal) part of the incident field from the incident (minus sign) and reflected (plus sign) parts of the acoustic disturbance, and (iii) two

forced-waved terms $b_{L,\pm}[i(\kappa_{L,i}^{\perp}\pm Q^{\perp})z]$, originating in the scattering of the *plasmonlike* (or irrotational) part of the incident field from the incident $(-)$ and reflected $(+)$ sound waves.

It should be mentioned that the factor $[(k_i^{\parallel})^2+(k_A^{\perp}\pm Q^{\perp})^2]^{-1}$ in Eq. (3.21) does not give poles in the upper half-plane at $k_A^{\perp}=ik_i^{\parallel}\pm Q^{\perp}$ since $N_L-N_T\propto(k_i^{\parallel})^2+(k_A^{\perp}\mp Q^{\perp})^2$ as these points are approached. This follows by realizing that we are in the realm of local optics close to the above points (see Sec. III C). The pole contributions to the scattered Stokes field are obtained by making the usual replacements $A\rightarrow S$, $u_i^{T1}(\vec{Q},\Omega)\rightarrow[u_i^{T1}(\vec{Q},\Omega)]^*$, $Q^{\parallel}\rightarrow -Q^{\parallel}$, and $\chi_{44}^{\omega_A,\omega_i,\Omega}\rightarrow\chi_{44}^{\omega_S,\omega_i,-\Omega}$ in all the relevant equations of Sec. III B.

C. Scattering in a fully degenerate plasma

To gain some further insight in the structure of the inelastically scattered field by analytical methods we shall in this section be concerned with heavily doped semiconductors and metals. Thus fully degenerate Fermi-Dirac statistics, i.e., $\partial f_0(\mathscr{E})/\partial\mathscr{E}=-\delta(\mathscr{E}-\mathscr{E}_F)$, δ being the Dirac δ function, and $\mathscr{E}_F$ the Fermi energy of the conduction electrons, will be applied. The use of degenerate statistics leads to the following expressions for the transverse and longitudinal linear conductivity response functions:[35,40,41]

$$\vec{\sigma}_T^{\,L}(k^{\parallel},k^{\perp},\omega)=\frac{3\sigma_0}{2(1-i\omega\tau)}\frac{1}{Z^2}\left[\frac{1+Z^2}{Z}\arctan Z-1\right] \tag{3.30}$$

and

$$\sigma_L^L(k^{\parallel},k^{\perp},\omega)=\frac{3\sigma_0}{1-i\omega\tau}\frac{1}{Z^2}\left[1-\frac{\arctan Z}{Z}\right]\times\left[1-\frac{1}{i\omega\tau}\left[1-\frac{\arctan Z}{Z}\right]\right]^{-1}, \tag{3.31}$$

where the nonlocal expansion parameter Z is given by

$$Z=\frac{[(k^{\parallel})^2+(k^{\perp})^2]^{1/2}v_F\tau}{1-i\omega\tau}\,. \tag{3.32}$$

One should emphasize that the conductivities in Eq. (3.29) and (3.30) have been obtained on the basis of a microscopic classical Boltzmann-equation calculation. If the characteristic de Broglie wavelength of the conduction electrons cannot be neglected one must, of course, replace the conductivity response functions above by the Lindhard quantum mechanical response functions.[44,45]

1. Branch-cut contributions

Let us return now to the expression (3.5) for the anti-Stokes scattered field inside the solid. Since $\arctan Z$ is singlevalued and analytic in the Z plane cut along the imaginary axis from i to $i\infty$ and $-i$ to $-i\infty$ it follows by combining Eqs. (3.5), (3.12)–(3.14), (3.21), and (3.30)–(3.32) that the integral in Eq. (3.5) has three (hyperbolic) branch cuts in the upper half part of the complex $k_A^{\perp}$ plane extending from the singularities at

$$k_A^{\perp}=\eta_A^{\perp}=i\left[(k_A^{\parallel})^2+\left[\frac{1-i\omega_A}{v_F\tau}\right]^2\right]^{1/2} \tag{3.33}$$

and

$$k_A^{\perp}=\eta_i^{\perp}\pm Q^{\perp}=i\left[(k_i^{\parallel})^2+\left[\frac{1-i\omega_i\tau}{v_F\tau}\right]^2\right]^{1/2}\pm Q^{\perp}\,, \tag{3.34}$$

toward infinity as shown in Fig. 1.

The detailed calculation of the branch-cut contributions to the scattered anti-Stokes field ($\vec{e}^{\,s}_{A,BC}$) inside the plasma will not be presented in this work. Emphasizing the spatial dependence of the field the results can be summarized via the formula

$$\vec{e}^{\,s}_{A,BC}(\vec{r},t)=-\vec{e}_y\exp[i(\vec{k}_A^{\parallel}\cdot\vec{r}-\omega_A t)]\times\left[e_0 z^{-2}\exp(-K_A z)+\sum_{+,-}(e_T^{\pm}z^{-2}+e_L^{\pm}z^{-3/2})\times\exp(-K_i^{\pm}z)\right], \tag{3.35}$$

where

$$K_A=\frac{1-i\omega_A\tau}{v_F\tau}[1+\tfrac{1}{2}(Z_A^{\parallel})^2] \tag{3.36}$$

and

$$K_i^{\pm}=\frac{1-i\omega_i\tau}{v_F\tau}[1+\tfrac{1}{2}(Z_i^{\parallel})^2]\pm iQ^{\perp}\,, \tag{3.37}$$

with the "parallel" components of the nonlocal expansion parameters given by $Z_i^{\parallel}=k_i^{\parallel}v_F\tau/(1-i\omega_i\tau)$ and $Z_A^{\parallel}=k_A^{\parallel}v_F\tau/(1-i\omega_A\tau)$. Note that the factor in front of the exponentials in Eq. (3.35) is proportional to z^{-2} for

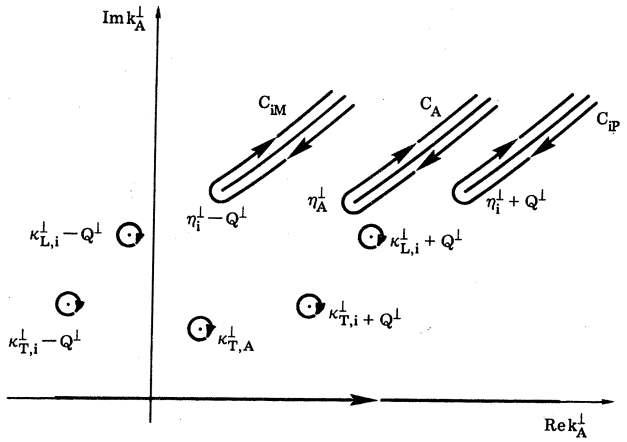

FIG. 1. Contours for evaluation of the scattered anti-Stokes field inside the solid-state plasma. The sum of the integral along the real $k_A^{\perp}$ axis, around the poles $\kappa_{T,A}^{\perp}$, $\kappa_{T,i}^{\perp}\pm Q^{\perp}$, and $\kappa_{L,i}^{\perp}\pm Q^{\perp}$, and along the three branch cuts C_A, C_{iM}, and C_{iP} must equal zero.

the terms (0,T) arising from the solenoidal part of the incident field, whereas it is proportional to $z^{-3/2}$ for the terms (L) of irrotational origin.

2. *Scattering of a coupled plasmariton-plasmon field: Fully nonlocal regime*

As pointed out in Sec. III B often merely a single solution exists to each of the dispersion relations $N_T(k^{\parallel},\kappa_T^{\perp},\omega)=0$ and $N_L(k^{\parallel},\kappa_L^{\perp},\omega)=0$. As typical examples are shown in Figs. 2 and 3 the real and imaginary parts of the transverse, i.e., $\kappa_T=\kappa_T(\omega),\kappa_T=[(k^{\parallel})^2+(\kappa_T^{\perp})^2]^{1/2}$, and the longitudinal, $\kappa_L=\kappa_L(\omega),\kappa_L=[(k^{\parallel})^2+(\kappa_L^{\perp})^2]^{1/2}$ dispersion relations of a free-electron-like metal (Al) and a heavily doped semiconductor (n-type InSb), respectively. The dispersion relations shown have been obtained on the basis of Eqs. (3.12), (3.13), (3.15), (3.16), and (3.30)–(3.32) using the following qualitatively representative material data at 300 K (Ref. 39). Al: $N_0=1.81\times10^{29}$ m^{-3}, $m^*/m_0=1.15$, $\tau=8.0\times10^{-15}$ sec, and $\chi^L=0$; n-type InSb: $N_0=1.20\times10^{24}$ m^{-3}, $m^*/m_0=3.20\times10^{-2}$, $\tau=4.0\times10^{-13}$ sec, and $\chi^L=14.68$.

For $\omega\tau\to\infty$, it appears from the longitudinal dispersion relation [Eq. (3.16)] that the nonlocal expansion parameter approaches i. Thus for $Z\to i$, one obtains $\kappa_L(\omega)\cong(\omega/v_F)+(i/v_F\tau)$, as indicated in Figs. 2 and 3. Note that the complex wave vector $\kappa_L(\omega)$ just equals the characteristic free-wave branch-cut wave vector at perpendicular incidence, i.e., $\kappa_L(\omega_A)=iK_A(\omega_A)$ for $\omega_A\tau\to\infty$ and $Z_A^{\parallel}=0$.

It can be shown[41] that the pole contribution to the scattered anti-Stokes field outside the solid, obtained on the basis of Eq. (3.4), is given by

$$E_{A0}^{s}(k_A^{\parallel},\omega_A)=\frac{-1}{k_{A0}^{\perp}+\kappa_{T,A}^{\perp}}\times\sum_{+,-}[(\kappa_{T,i}^{\perp}\pm Q^{\perp}-\kappa_{T,A}^{\perp})b_{T,\pm}+(\kappa_{L,i}^{\perp}\pm Q^{\perp}-\kappa_{T,A}^{\perp})b_{L,\pm}]\,. \quad (3.38)$$

Outside the solid, the ratio between the magnitudes of the time-averaged ($\langle\ \rangle_T$) Poynting vectors of the s-polarized anti-Stokes field ($\vec{S}_{A0}^{\,s}$) and the p-polarized incident field ($\vec{S}_{i0}^{\,p}$) becomes

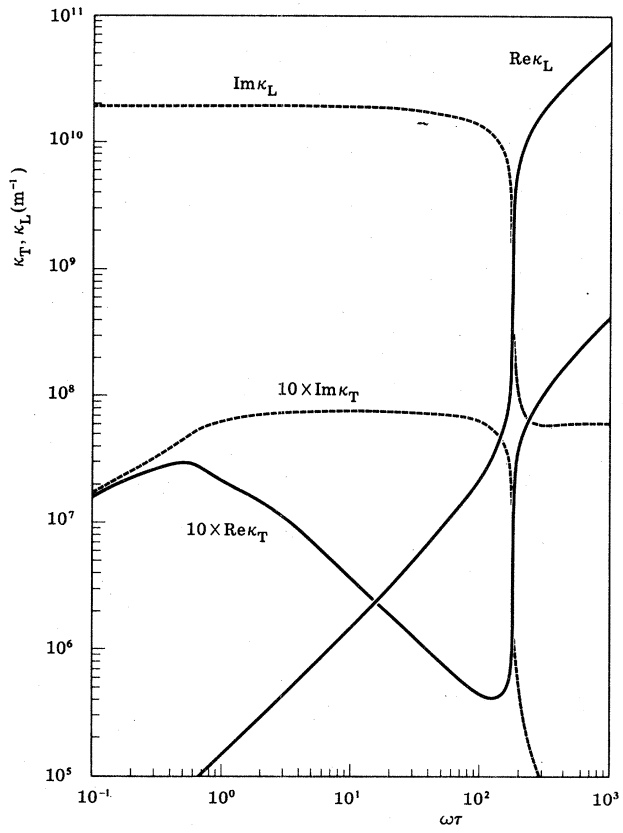

FIG. 2. Real (solid curves) and imaginary (dashed curves) parts of the transverse (κ_T) and longitudinal (κ_L) wave vectors of the electromagnetic field in Al as functions of the dimensionless optical frequency $\omega\tau$. Note that $10\times\kappa_T$ has been plotted in the figure. With the adopted relaxation time $\tau=8.0\times10^{-15}$ sec; the positions of the 0.63-μm He-Ne laser line and the 10.6-μm CO_2 line are at $\omega\tau\cong24$ and 1.4, respectively.

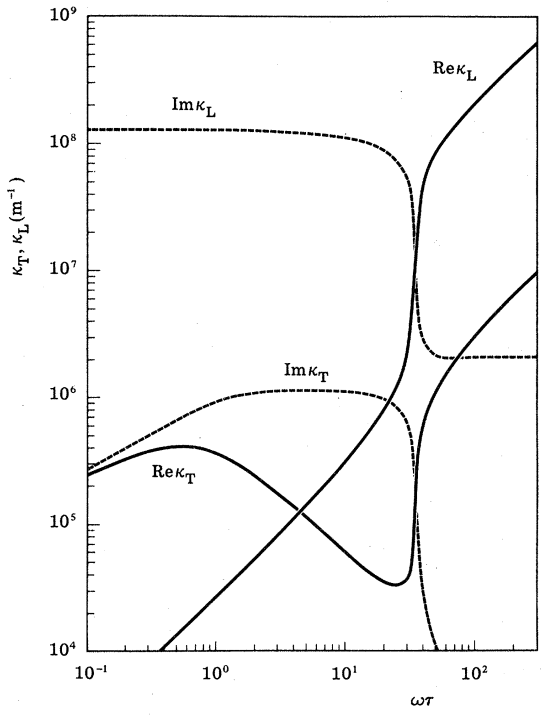

FIG. 3. Real (solid curves) and imaginary (dashed curves) parts of the transverse (κ_T) and longitudinal (κ_L) wave vectors of the electromagnetic field in n-type InSb as functions of the dimensionless optical frequency $\omega\tau$. With the adopted relaxation time $\tau=4.0\times10^{-13}$ sec, the positions of the 10.6-μm CO_2 laser line and the 337-μm HCN line are at $\omega\tau\cong71$ and 2.2, respectively. The band edge ($\sim$0.16 eV at 300 K) corresponds to $\omega\tau\cong98$.

$$\frac{|\langle \vec{S}^{s}_{A0}(k_A^{\parallel},\omega_A)\rangle_T|}{|\langle \vec{S}^{p}_{i0}(k_i^{\parallel},\omega_i)\rangle_T|}=\left[\frac{\omega_A}{c_0}\right]^4 |u_i^{T1}(\vec{Q},\Omega)|^2 |\chi_{44}^{\omega_A,\omega_i,\Omega}|^2 \left|\frac{t^p(k_i^{\parallel},\omega_i)}{k_{A0}^{\perp}+\kappa_{T,A}^{\perp}}\right|^2$$
$$\times\left|\mathscr{R}_T(k_i^{\parallel},\kappa_{T,i}^{\perp},\omega_i)\frac{\kappa_{T,i}^{\perp}(k_i^{\parallel}Q^{\perp}-\kappa_{T,i}^{\perp}Q^{\parallel})}{(k_i^{\parallel})^2+(\kappa_{T,i}^{\perp})^2}\sum_{+,-}\frac{\kappa_{T,i}^{\perp}\pm Q^{\perp}-\kappa_{T,A}^{\perp}}{N_T(k_A^{\parallel},\kappa_{T,i}^{\perp}\pm Q^{\perp},\omega_A)}\right.$$
$$\left.-\mathscr{R}_L(k_i^{\parallel},\kappa_{L,i}^{\perp},\omega_i)\frac{k_i^{\parallel}(k_i^{\parallel}Q^{\parallel}+\kappa_{L,i}^{\perp}Q^{\perp})}{(k_i^{\parallel})^2+(\kappa_{L,i}^{\perp})^2}\sum_{+,-}\frac{\kappa_{L,i}^{\perp}\pm Q^{\perp}-\kappa_{T,A}^{\perp}}{N_T(k_A^{\parallel},\kappa_{L,i}^{\perp}\pm Q^{\perp},\omega_A)}\right|^2, \tag{3.39}$$

with $t^p(k_i^{\parallel},\omega_i)$ given by

$$t^p(k_i^{\parallel},\omega_i)=-i\left[\frac{\omega_i(k_i^{\parallel})^2}{c_0k_{i0}^{\perp}[(k_i^{\parallel})^2+(\kappa_{L,i}^{\perp})^2]}\mathscr{R}_L(k_i^{\parallel},\kappa_{L,i}^{\perp},\omega_i)+\left[\frac{c_0\kappa_{T,i}^{\perp}}{\omega_i}+\frac{\omega_i(\kappa_{T,i}^{\perp})^2}{c_0k_{i0}^{\perp}[(k_i^{\parallel})^2+(\kappa_{T,i}^{\perp})^2]}\right]\mathscr{R}_T(k_i^{\parallel},\kappa_{T,i}^{\perp},\omega_i)\right]^{-1}. \tag{3.40}$$

3. *Scattering of a coupled plasmariton-plasmon field: Near-local regime*

A numerical calculation of the scattered anti-Stokes Poynting vector in Eq. (3.39) is impeded by the fact that the nonlocal expressions for the linear conductivity response functions [Eqs. (3.30) and (3.31)] are quite complicated. However, for optical frequencies around the plasma edge Eq. (3.39) can be simplified considerably. Thus it appears from Fig. 4 that the magnitude of the longitudinal nonlocal expansion parameter Z_L is somewhat less than unity close to the plasma frequency. This makes it appropriate to utilize a Taylor-series expansion around $Z_L=0$ for σ_L^L. It is known[39] that for Al and n-type InSb a Taylor series expansion to lowest order in Z_T is appropriate in the study of *linear* optical properties associated with the solenoidal component of the electromagnetic field not only around the plasma edge, but over the entire optical frequency spectrum.

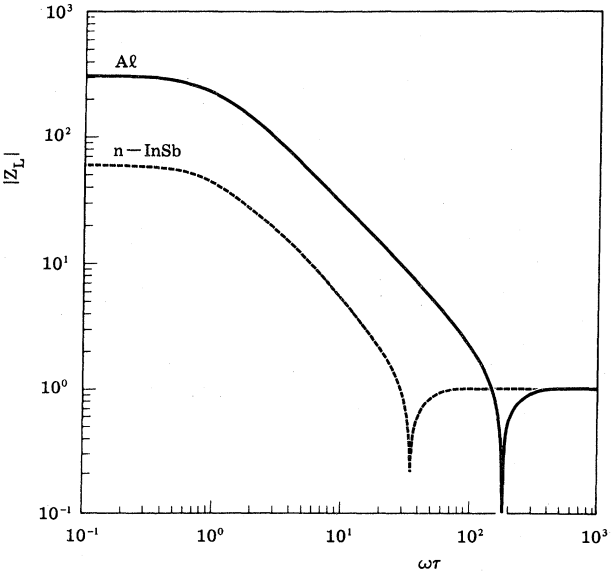

FIG. 4. Magnitude of the longitudinal nonlocal expansion parameter Z_L as a function of the dimensionless optical frequency $\omega\tau$ in fully degenerate Al (solid curve) and n-type InSb (dashed curve) plasmas. The deep minima are located at the respective plasma edges.

Thus in the so-called near-local regime where the conductivity response functions are expanded to lowest, i.e., second order in Z_L and Z_T the dispersion relations take the form

$$\kappa_M^{\perp}(k^{\parallel},\omega)=\left[\frac{\alpha_M(k^{\parallel},\omega)}{\beta_M(k^{\parallel},\omega)}\right]^{1/2},\quad \mathrm{Im}\kappa_M^{\perp}>0,\quad M=\mathrm{L,T} \tag{3.41}$$

where

$$\alpha_T(k^{\parallel},\omega)=\left[\frac{\omega}{c_0}\right]^2[1+\chi^L(\omega)]+i\mu_0\omega\frac{\sigma_0}{1-i\omega\tau}\times\left[1-\frac{1}{5}\left[\frac{k^{\parallel}v_F\tau}{1-i\omega\tau}\right]^2\right]-(k^{\parallel})^2, \tag{3.42}$$

$$\beta_T(k^{\parallel},\omega)=1+\frac{i\mu_0\omega\sigma_0(v_F\tau)^2}{5(1-i\omega\tau)^3}, \tag{3.43}$$

$$\alpha_L(k^{\parallel},\omega)=\left[\frac{\omega}{c_0}\right]^2[1+\chi^L(\omega)]+i\mu_0\omega\frac{\sigma_0}{1-i\omega\tau}\left[1-\left[\frac{3}{5}-\frac{1}{3i\omega\tau}\right]\times\left[\frac{k^{\parallel}v_F\tau}{1-i\omega\tau}\right]^2\right], \tag{3.44}$$

and

$$\beta_L(k^{\parallel},\omega)=\frac{i\mu_0\omega\sigma_0(v_F\tau)^2}{(1-i\omega\tau)^3}\left[\frac{3}{5}-\frac{1}{3i\omega\tau}\right]. \tag{3.45}$$

For brevity the compact notation $\kappa_T^{\perp}\equiv\kappa_{T,i}^{\perp}$ or $\kappa_{T,A}^{\perp}$, $\kappa_L^{\perp}\equiv\kappa_{L,i}^{\perp}$ or $\kappa_{L,A}^{\perp}$, and $(k^{\parallel},\omega)\equiv(k_i^{\parallel},\omega_i)$ or $(k_A^{\parallel},\omega_A)$ has been introduced.

In Figs. 5 (Al) and 6 (n-type InSb) we have, for frequencies around the plasma edge, compared the irrotational dispersion relation obtained on the basis of the near-local

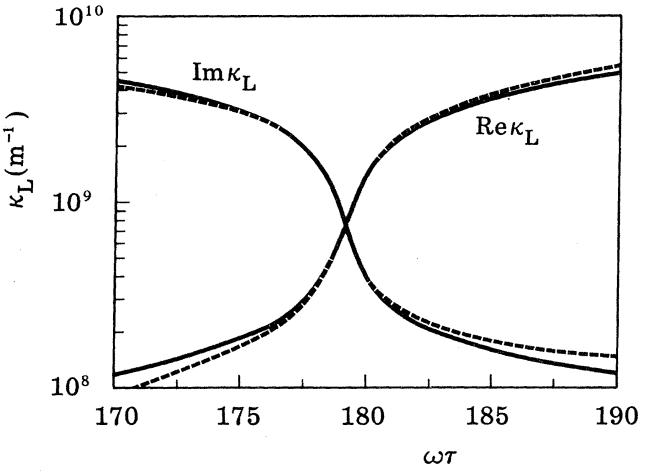

FIG. 5. Real and imaginary parts of the longitudinal wave vector of the electromagnetic field in Al as functions of the dimensionless optical frequency $\omega\tau$ for frequencies around the plasma edge. The solid curves correspond to a nonlocal calculation, the dashed curves to a near-local approximation.

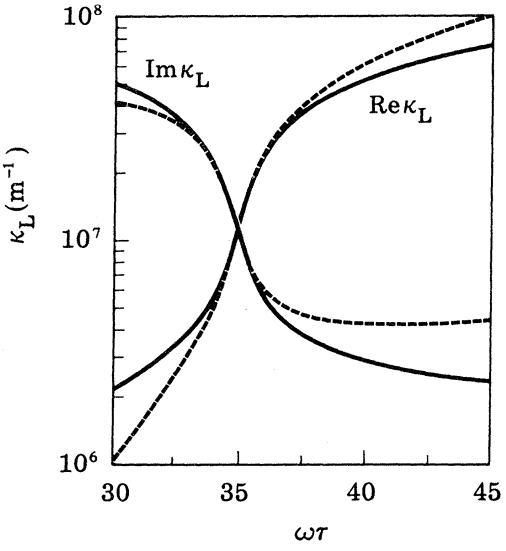

FIG. 6. Real and imaginary parts of the longitudinal wave vector of the electromagnetic field in n-type InSb as functions of the dimensionless optical frequency $\omega\tau$ for frequencies close to the plasma edge. The solid and dashed curves correspond to nonlocal and near-local calculations, respectively.

formula in Eq. (3.41) with that obtained via the fully nonlocal model. Explicitly, one can estimate (see also Ref. 39) that the near-local approximation holds for $|Z_L|^2 \lesssim 10^{-1}$, i.e., in the ranges $174 \lesssim \omega\tau \lesssim 185$ (Al) and $34 \lesssim \omega\tau \lesssim 36$ (n-type InSb). The local approximation which holds for $|Z_L|^2 \lesssim 10^{-2}$, apart from at the plasma edge in Al, cannot be met anywhere in the spectra of Al and n-type InSb.

In the near-local regime readily one obtains

$$N_T(k_A^{\parallel},\kappa^{\perp}_{,i}\pm Q^{\perp},\omega_A)=\alpha_T(k_A^{\parallel},\omega_A)-(\kappa^{\perp}_{,i}\pm Q^{\perp})^2\beta_T(k_A^{\parallel},\omega_A), \tag{3.46}$$

where $\kappa^{\perp}_{,i}\equiv\kappa^{\perp}_{T,i}$ or $\kappa^{\perp}_{L,i}$. By inserting Eqs. (3.41) and (3.46) into Eq. (3.39) and calculating the appropriate residues, the final expression for the ratio between the magnitude of the time-averaged Poynting vectors $\langle\vec{S}^s_{A0}\rangle_T$ and $\langle\vec{S}^p_{i0}\rangle_T$ takes the form

$$\begin{aligned}\frac{|\langle\vec{S}^s_{A0}(k_A^{\parallel},\omega_A)\rangle_T|}{|\langle\vec{S}^p_{i0}(k_i^{\parallel},\omega_i)\rangle_T|}=&\left[\frac{\omega_A}{c_0}\right]^4|u_i^{T1}(\vec{Q},\Omega)|^2\,|t^p(k_i^{\parallel},\omega_i)|^2\left|\frac{\beta_T^{-1}(k_A^{\parallel},\omega_A)}{k^{\perp}_{A0}+\kappa^{\perp}_{T,A}}\right|^2\\&\times\left|\beta_T^{-1}(k_i^{\parallel},\omega_i)\frac{Q^{\parallel}\kappa^{\perp}_{T,i}-Q^{\perp}k_i^{\parallel}}{(k_i^{\parallel})^2+(\kappa^{\perp}_{T,i})^2}\frac{\kappa^{\perp}_{T,i}+\kappa^{\perp}_{T,A}}{(\kappa^{\perp}_{T,i}+\kappa^{\perp}_{T,A})^2-(Q^{\perp})^2}+\beta_L^{-1}(k_i^{\parallel},\omega_i)\frac{k_i^{\parallel}}{\kappa^{\perp}_{L,i}}\right.\\&\left.\times\frac{Q^{\parallel}k_i^{\parallel}+Q^{\perp}\kappa^{\perp}_{L,i}}{(k_i^{\parallel})^2+(\kappa^{\perp}_{L,i})^2}\frac{\kappa^{\perp}_{L,i}+\kappa^{\perp}_{T,A}}{(\kappa^{\perp}_{L,i}+\kappa^{\perp}_{T,A})^2-(Q^{\perp})^2}\right|^2\end{aligned} \tag{3.47}$$

in the near-local regime. The corresponding formula for $t^p(k_i^{\parallel},\omega_i)$ is given by

$$t^p(k_i^{\parallel},\omega_i)=2i\left[\frac{c_0}{\omega_i}\beta_T^{-1}(k_i^{\parallel},\omega_i)+\left[\frac{(k_i^{\parallel})^2(\kappa^{\perp}_{L,i})^{-1}\beta_L^{-1}(k_i^{\parallel},\omega_i)}{(k_i^{\parallel})^2+(\kappa^{\perp}_{L,i})^2}+\frac{\kappa^{\perp}_{T,i}\beta_T^{-1}(k_i^{\parallel},\omega_i)}{(k_i^{\parallel})^2+(\kappa^{\perp}_{T,i})^2}\right]\frac{\omega_i}{c_0k^{\perp}_{i0}}\right]^{-1}. \tag{3.48}$$

4. *Phase matching and resonance scattering*

To discuss the structure of the scattered anti-Stokes intensity we note that

$$-\beta_T(k_A^{\parallel},\omega_A)\sum_{+,-}\frac{\kappa^{\perp}_{,i}\pm Q^{\perp}-\kappa^{\perp}_{T,A}}{N_T(k_A^{\parallel},\kappa^{\perp}_{,i}\pm Q^{\perp},\omega_A)}=\sum_{+,-}[\mathrm{Re}(\kappa^{\perp}_{,i}+\kappa^{\perp}_{T,A})\pm Q^{\perp}+i\,\mathrm{Im}(\kappa^{\perp}_{,i}+\kappa^{\perp}_{T,A})]^{-1}, \tag{3.49}$$

in the near-local regime. As in Sec. III C 3 we have used the compact notation $\kappa^{\perp}_{,i} \equiv \kappa^{\perp}_{\mathrm{T},i}$ or $\kappa^{\perp}_{\mathrm{L},i}$.

Phase matching occurs when

$$\mathrm{Re}\kappa^{\perp}_{,i} + \mathrm{Re}\kappa^{\perp}_{\mathrm{T},A} \pm Q^{\perp} = 0 , \tag{3.50}$$

where the plus sign corresponds to matching with the reflected sound wave. The four phase-matched processes given by Eq. (3.50) are illustrated schematically in Fig. 7. Two of the processes describe phase matching of the solenoidal and the irrotational parts of the field with the incident acoustic mode, respectively; the two other processes stem from matching with the reflected sound field. To obtain a phase matched anti-Stokes scattering process in *reflection* spectroscopy one must have $\mathrm{Re}\kappa^{\perp}_{,i} \pm Q^{\perp} < 0$. Since $\mathrm{Re}\kappa^{\perp}_{,i} > 0$ and $Q^{\perp} > 0$, it immediately follows that only scattering from the incident mode (minus sign) can cause phase matching in reflection spectroscopy (see Fig. 7). The reflected acoustic field, of course, can give resonance in Stokes scattering. According to Eq. (3.22) one must demand $\mathrm{Im}\kappa^{\perp}_{\mathrm{T},A} > 0$. This implies $\mathrm{Re}\kappa^{\perp}_{\mathrm{T},A} > 0$ consistent with the requirement $-\mathrm{Re}\kappa^{\perp}_{\mathrm{T},A} = \mathrm{Re}\kappa^{\perp}_{,i} - Q^{\perp} < 0$.

Normally, the resonance with the irrotational and the solenoidal parts of the incoming field are well separated (see Sec. V). If so, the condition for maximum intensity, taken as a function of the *magnitude* of Q, approximately is given by

$$(\mathrm{Re}\kappa^{\perp}_{,i} + \mathrm{Re}\kappa^{\perp}_{\mathrm{T},A})^2 + (\mathrm{Im}\kappa^{\perp}_{,i} + \mathrm{Im}\kappa^{\perp}_{\mathrm{T},A})^2 = (Q^{\perp})^2 , \tag{3.51}$$

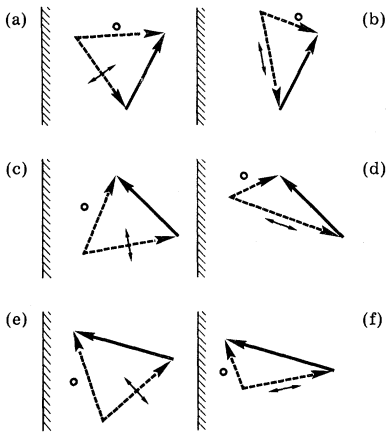

FIG. 7. Schematic diagrams showing different phase matched anti-Stokes scattering processes with p-polarized incident light. The T1 polarized acoustic wave vector is indicated by the solid arrow, the optical wave vectors of the incident and scattered fields by broken arrows. The direction of polarization of light is shown by thin double arrows and circles. (a)—(d) and (e)—(f) correspond to phase matching in transmission and reflection spectroscopy, respectively. In (a) and (b) phase matching of the solenoidal and irrotational parts of the incident field with the incident acoustic mode is shown. The (c) and (d) diagrams stem from matching with the reflected acoustic field. As illustrated in (e) and (f) phase matching with the solenoidal or irrotational parts of the incident light field in reflection spectroscopy only can occur via the incident sound field.

for incident and reflected sound waves propagating at an arbitrary fixed angle with respect to the surface. In the transparent regime, i.e., for $\mathrm{Im}\kappa^{\perp}_{,i} \ll \mathrm{Re}\kappa^{\perp}_{,i}$, Eq. (3.51) reduces exactly to the phase-matching condition in Eq. (3.50).

Furthermore, when opacity effects are unimportant so that $\kappa^{\perp}_{\mathrm{T},i}$ and $\kappa^{\perp}_{\mathrm{L},i}$, are essentially real quantities the inelastic scattering from the T mode vanishes for $Q^{\parallel}\kappa^{\perp}_{\mathrm{T},i} = Q^{\perp}k^{\parallel}_{i}$ and the scattering from the L mode for $Q^{\parallel}k^{\parallel}_{i} = -Q^{\perp}\kappa^{\perp}_{\mathrm{L},i}$. This conclusion holds even in the fully nonlocal regime [see Eq. (3.39)]. Remembering that (i) the solenoidal and irrotational modes become purely transverse and longitudinal in the transparent regime, and (ii) total and specular scattering of the acoustic wave at the surface makes the solid-state plasma equal to an infinite medium as far as elastic properties are concerned, the zeros in the scattering intensity are related to geometrical scattering configurations where the polarization of the electromagnetic mode in consideration is perpendicular to the acoustic wave vector and the acoustic displacement as shown in Fig. 8.

To obtain the condition for a local maximum in the scattering intensity in the fully nonlocal case one makes a Taylor expansion of $N_{\mathrm{T}}(k^{\parallel}_{A}, \kappa^{\perp}_{,i} \pm Q^{\perp}, \omega_A)$ around $\kappa^{\perp}_{\mathrm{T},A}$. Remembering that $N_{\mathrm{T}}(k^{\parallel}_{A}, \kappa^{\perp}_{\mathrm{T},A}, \omega_A) = 0$ one gets to second-order

$$\frac{1}{4}\frac{\partial^2 N_{\mathrm{T}}(k^{\parallel}_{A}, k^{\perp}_{A}, \omega_A)}{(\partial k^{\perp}_{A})^2}\bigg|_{k^{\perp}_{A}=\kappa^{\perp}_{\mathrm{T},A}} \sum_{+,-} \frac{\kappa^{\perp}_{,i} \pm Q^{\perp} - \kappa^{\perp}_{\mathrm{T},A}}{N_{\mathrm{T}}(k^{\parallel}_{A}, \kappa^{\perp}_{,i} \pm Q^{\perp}, \omega_A)}$$

$$\cong \frac{D(k^{\parallel}_{A}, \kappa^{\perp}_{\mathrm{T},A}, \omega_A) + \kappa^{\perp}_{,i} - \kappa^{\perp}_{\mathrm{T},A}}{[D(k^{\parallel}_{A}, \kappa^{\perp}_{\mathrm{T},A}, \omega_A) + \kappa^{\perp}_{,i} - \kappa^{\perp}_{\mathrm{T},A}]^2 - (Q^{\perp})^2} , \tag{3.52}$$

where

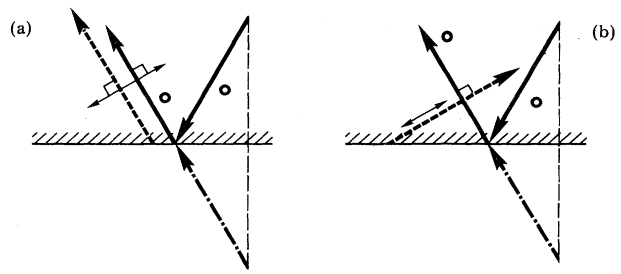

FIG. 8. Schematic diagrams showing combined wave-vector and polarization geometries in the transparent frequency regime where the acousto-optic scattering intensity vanishes. In (a) the polarization (thin double arrow) of the solenoidal part of the p-polarized incident electromagnetic field (dashed wave vector) is perpendicular to the acoustic polarization (circle), the wave vector of the reflected sound field (solid arrow), and the mirror image of the incident acoustic wave vector in the surface plane (dashed-dotted arrow). Thus, in (a) the scattering from the T mode vanishes. In (b) a configuration in which the scattering from the irrotational (L mode) part of the incident electromagnetic field disappears is shown.

$$D(k_A^{\parallel},\kappa_{T,A}^{\perp},\omega_A)=2\frac{\left.\frac{\partial N_T(k_A^{\parallel},k_A^{\perp},\omega_A)}{\partial k_A^{\perp}}\right|_{k_a^{\perp}=\kappa_{T,A}^{\perp}}}{\left.\frac{\partial^2 N_T(k_A^{\parallel},k_A^{\perp},\omega_A)}{(\partial k_A^{\perp})^2}\right|_{k_A^{\perp}=\kappa_{T,A}^{\perp}}} . \tag{3.53}$$

By combining Eqs. (3.39) and (3.52) the irrotational and solenoidal resonances, taken as functions of the magnitude of the acoustic wave vector, approximately occur when

$$|D(k_A^{\parallel},\kappa_{T,A}^{\perp},\omega_A)+\kappa_{,i}^{\perp}-\kappa_{T,A}^{\perp}|^2=(Q^{\perp})^2 . \tag{3.54}$$

In the near-local regime the resonance condition in Eq. (3.54) is reduced to that given in Eq. (3.51), since Eq. (3.46) implies $D=2\kappa_{T,A}^{\perp}$.

IV. SCATTERING OF AN *s*-POLARIZED INCIDENT FIELD

In the preceding section a detailed treatment of the anti-Stokes scattering of a *p*-polarized incident electromagnetic field has been presented. By imitating this investigation, albeit tedious, it is a straightforward matter to analyze in a quantitative manner the inelastic scattering of an *s*-polarized incident field. However, we shall desist from doing this in the present paper and merely stress a few qualitative results of such an analysis.

Inside the solid-state plasma the anti-Stokes scattered field becomes *p* polarized and is given by

$$\vec{E}_A^{\,p}(\vec{r},t)=\exp[i(\vec{k}_A^{\parallel}\cdot\vec{r}-\omega_A t)]\sum_{+,-}\sum_n\{\vec{a}_{T,\pm}^{\,n}\exp(i\kappa_{T,A}^{\perp,n}z)+\vec{a}_{L,\pm}^{\,n}\exp(i\kappa_{L,A}^{\perp,n}z)+\vec{b}_{T,\pm}^{\,n}\exp[i(\kappa_{T,i}^{\perp,n}\pm Q^{\perp})z]\}+\cdots , \tag{4.1}$$

where the ellipsis includes unspecified branch-cut contributions and the vectors $\vec{a}_{T,\pm}^{\,n}$, $\vec{a}_{L,\pm}^{\,n}$, and $\vec{b}_{T,\pm}^{\,n}$ are confined to the *x*-*z* plane. The interpretation of the result in Eq. (4.1) is easy. Thus, apart from a summation (n) over solutions to the dispersion relations in Eqs. (3.15) and (3.16) and branch-cut contributions, the field is composed of (i) solenoidal,

$$(\vec{a}_{T,+}^{\,n}+\vec{a}_{T,-}^{\,n})\exp(i\kappa_{T,A}^{\perp,n}z) ,$$

and irrotational,

$$(\vec{a}_{L,+}^{\,n}+\vec{a}_{L,-}^{\,n})\exp(i\kappa_{L,A}^{\perp,n}z) ,$$

free-wave contributions, which are necessary for the fulfillment of the boundary conditions of the scattered field at the surface, and (ii) two *forced-wave* contributions,

$$\vec{b}_{T,\pm}^{\,n}\exp[i(\kappa_{T,i}^{\perp,n}\pm Q^{\perp})z] ,$$

originating in the scattering of the incident plasmariton field from the incident (−) and reflected (+) sound waves. Schematic illustrations of the *p*-*s* and *s*-*p* scattering kinematics are shown in Figs. 9 and 10.

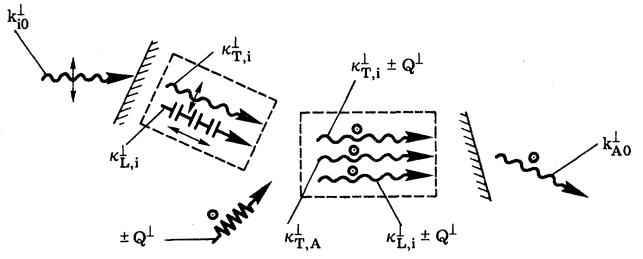

FIG. 9. Schematic illustration of the acousto-optic anti-Stokes *p*-*s* scattering kinematics. The acoustic, the plasmonlike (irrotational), and the plasmaritonlike (solenoidal) wave vectors have been indicated by different types of arrows. The thin arrows and the circles denote the state of polarization of the field associated with a given mode. Each wave vector has been labeled with its component perpendicular to the surface.

Let us assume that only $n=1$ contributes to the field pattern inside the plasma. If so, in *p*-*s* scattering the number of components necessary to describe the state of polarization of light is $2\times2=4$ for the incident field and $2+2+1=5$ for the anti-Stokes scattered field, i.e., in total 9. For the *s*-*p* scattering process the corresponding number of components is 1 for the incident field and $2\times2+2+2=8$ for the scattered field. Hence, altogether we have 9 as for the *p*-*s* process.

V. NUMERICAL RESULTS

To emphasize the importance of nonlocal optical effects for acousto-optic light scattering studies in metals and semiconductors we shall present some quantitative numerical calculations of anti-Stokes intensities in this section. Our results, apart from a slight change discussed below, will be expressed in terms of the function

$$I^{p\to s}(\theta,\phi,\omega_i,\Omega)=\frac{N}{|u_i^{T1}(\vec{Q},\Omega)|^2|\chi_{44}^{\omega_A,\omega_i,\Omega}|^2}\times\frac{|\langle\vec{S}_{A0}^{\,s}(k_A^{\parallel},\omega_A)\rangle_T|}{|\langle\vec{S}_{i0}^{\,p}(k_i^{\parallel},\omega_i)\rangle_T|} , \tag{5.1}$$

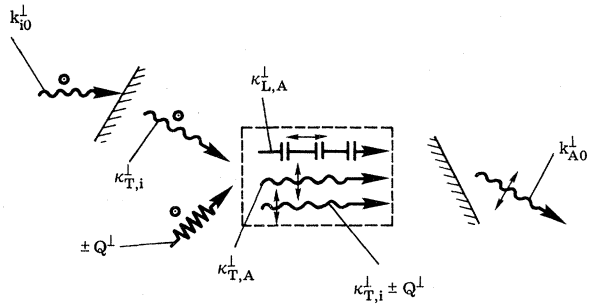

FIG. 10. Schematic illustration of the acousto-optic anti-Stokes *s*-*p* scattering kinematics. The wave-vector and polarization symbols and the labeling of the wave vectors are as in Fig. 9.

where N is an appropriate normalization factor for the spectra. The quantities $\phi=\arctan(Q^{\parallel}/Q^{\perp})$ and $\theta=\arctan(k_i^{\parallel}/k_{i0}^{\perp})$ denote the angles of incidence towards the surface of the acoustic and the incident electromagnetic waves, respectively.

In conventional local theories of acousto-optic scattering one can neglect elastic dispersion effects since the acoustic wave vectors involved are much smaller than a characteristic Brillouin-zone boundary wave vector. However, resonance scattering via the irrotational part of the electromagnetic field involves acoustic wave vectors of magnitudes comparable to the extension of the Brillouin zone. Hence, at least for metals as well as we shall see, one must incorporate the phonon dispersion effects via a wave-vector dependent phase velocity $V_p^{\mathrm{T1}}(\vec{Q})$, i.e.,

$$\Omega=V_p^{\mathrm{T1}}(\vec{Q})Q\ . \tag{5.2}$$

In consequence of this we shall express $I^{p\to s}$ in terms of Q instead of Ω. This is very adequate since Ω occurs in the Poynting vector ratios in Eqs. (3.39) and (3.47) only through ω_A, $\kappa_{\mathrm{T},A}^{\perp}$, and $N_{\mathrm{T}}(k_A^{\parallel},\kappa_{,i}^{\perp}\pm Q^{\perp},\omega_A)$. Since $\Omega\ll\omega_i$ these quantities are almost independent of the precise Ω value. In the calculations of $I^{p\to s}$ presented below we have used $V_p^{\mathrm{T1}}=2.30\times10^3$ m/sec (n-type InSb) (Ref. 46) and $V_p^{\mathrm{T1}}=3.22\times10^3$ m/sec (Al) (Ref. 3) for *all* values of Q.

In the following we shall limit ourselves to cases where the angles θ and ϕ are kept fixed. We choose $\phi=0°$ corresponding to perpendicular incidence of the acoustic wave on the surface ($Q^{\parallel}=0$). To obtain anti-Stokes scattering one must demand $k_i^{\parallel}\neq0$ for $Q^{\parallel}=0$ according to Eq. (3.39). We take $\theta=5°$.

Let us consider the acousto-optic scattering in n-type InSb. In Fig. 11 is shown $I^{p\to s}$ as a function of the acoustic wave vector $Q^{\perp}=Q$ ($Q^{\parallel}=0$) for $\omega_i\tau=50$, i.e., for a frequency above the plasma edge, $\omega_p\tau\cong35$. The two peaks at $Q^{\perp}\cong2.36\times10^6$ m^{-1} ($\Omega\cong5.43\times10^9$ Hz) and 9.17×10^7 m^{-1} (2.11×10^{11} Hz) correspond to the resonances with the plasmariton and plasmonlike parts of the electromagnetic field, respectively. The numbers in the parentheses are the associated acoustic frequencies. Since the acoustic wave vectors are small in comparison with the reciprocal lattice constant, these frequencies lie in the elastically nondispersive regime. The half widths of the peaks are $\Delta Q^{\perp}\cong0.04\times10^6$ m^{-1} ($\Delta\Omega\cong0.09\times10^9$ Hz) and 0.43×10^7 m^{-1} (0.11×10^{11} Hz), respectively. The normalization factor N has been chosen in this and subsequent figures on n-type InSb so that $I^{p\to s}=1$ at the plasmariton resonance corresponding to $\omega_i\tau=50$, $\phi=0°$, and $\theta=5°$. Note that the ratio between the L- and T-mode intensities at resonance is $\sim\frac{1}{40}$ at $\omega_i\tau=50$. The skew distribution of the intensity around the peaks, showing the most rapid decay on the low-wave-vector (or frequency) side, stems from the presence of acoustic phonon reflection at the crystal surface in agreement with the calculations by Dervisch and Loudon.[7] For comparison also we have shown a calculation of $I^{p\to s}$ based on the near-local approximation [Eq. (3.47)]. As expected, the near-local model predicts the localization, the intensity, and the shape of the plasmariton resonance quite accurately. The plasmon

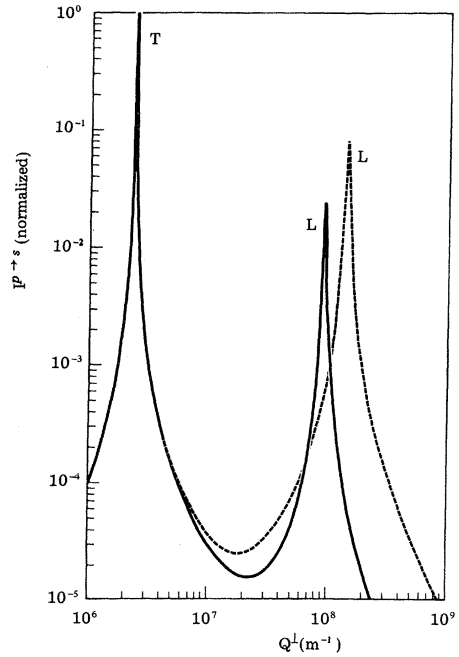

FIG. 11. Normalized anti-Stokes intensity $I^{p\to s}$ in n-type InSb for the p-s scattering configuration as a function of the acoustic wave vector $Q^{\perp}$. The dimensionless optical frequency has the value $\omega_i\tau=50$. The optical and acoustic angles of incidence are $\theta=5°$ and $\phi=0°$, respectively. The solid curve represents a nonlocal and the broken curve a near-local calculation. The plasmaritonlike and plasmonlike resonances have been denoted by T and L, respectively.

resonance is shifted towards higher wave vectors, i.e., $Q^{\perp}\cong1.40\times10^8$ m^{-1} ($\Omega\cong3.22\times10^{11}$ Hz) as one would guess from the plasmonlike dispersion relation in Fig. 6. The halfwidth has increased to $\Delta Q^{\perp}\cong0.09\times10^8$ m^{-1} ($\Delta\Omega\cong0.21\times10^{11}$ Hz) and the peak intensity by a factor of ~3.3. A numerical calculation shows that the localizations of the L and T resonances are in complete agreement with the prediction made in Eq. (3.54). In the near-local model the peak positions coincide with those calculated by means of Eq. (3.51).

In Fig. 12 is shown $I^{p\to s}$ as a function of $Q^{\perp}$ for three optical frequencies around the plasma edge. The results presented are based on the nonlocal approach. However, since the nonlocal expansion parameter is somewhat smaller than unity for frequencies close to the plasma edge (see Fig. 4), calculations based on the near-local approximation only deviate slightly from those shown in Fig. 12. Note that close to the edge the strengths of the plasmariton and plasmon resonances are of the same order of magnitude. Approaching the plasma frequency ($\omega_p\tau=35$) from below and above, the peak positions of the L and T modes are displaced towards lower wave vectors ($Q^{\perp}$) and hence frequencies (Ω). Furthermore, the linewidths increase drastically as one goes to frequencies below the plasma edge.

Now, let us consider the acousto-optic scattering from a single acoustic mode taken as a function of the frequency of light. In Fig. 13 is shown the normalized scattered intensity $I^{p\to s}$ for $Q^{\perp}=10^6$ m^{-1} ($\Omega=2.3$ GHz) and $Q^{\perp}=2\times10^6$ m^{-1} ($\Omega\cong4.6$ GHz) vs $\omega_i\tau$. The resonances

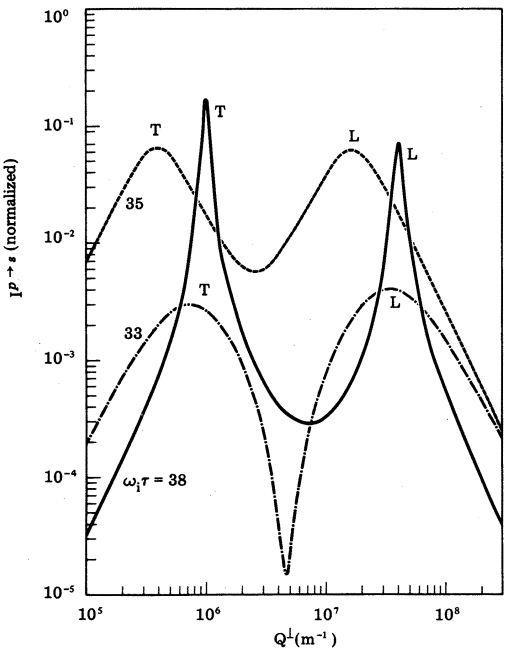

FIG. 12. Normalized anti-Stokes intensity $I^{p\to s}$ in n-type InSb for the p-s scattering configuration as a function of the acoustic wave vector $Q^\perp$ for the three different dimensionless optical frequencies $\omega_i\tau=33$, 35, and 38 around the plasma edge. The optical and acoustic angles of incidence are $\theta=5°$ and $\phi=0°$, respectively. The plasmaritonlike and plasmonlike resonances have been labeled by T and L, respectively. The nonlocal and near-local models give essentially the same result.

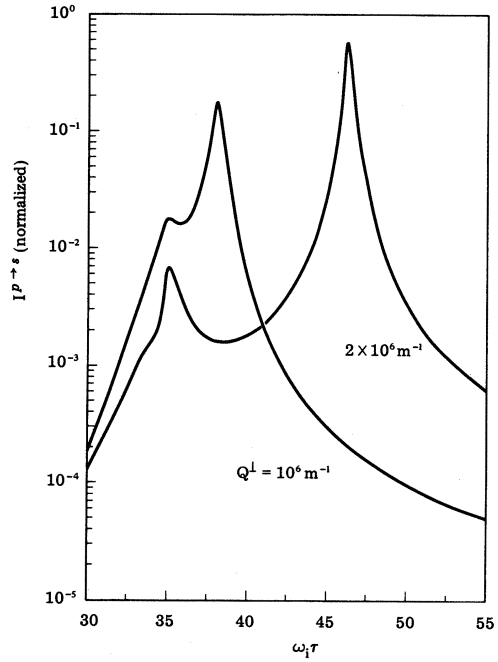

FIG. 13. Normalized anti-Stokes intensity $I^{p\to s}$ in n-type InSb for the p-s scattering configuration as a function of the dimensionless optical frequency $\omega_i\tau$ for two acoustic wave vectors $Q^\perp=10^6$ m^{-1} and 2×10^6 m^{-1}. The optical and acoustic angles of incidence are $\theta=5°$ and $\phi=0°$, respectively. The resonances essentially stem from the interaction with the plasmaritonlike part of the incident field. Nonlocal and near-local calculations of $I^{p\to s}$ give the same result.

at $\omega_i\tau\cong38.0$ and 46.2 stem from the interaction with the plasmaritonlike part of the electromagnetic field, mainly. As expected from the plasmariton dispersion relation in Fig. 3 the resonance is displaced toward higher $\omega_i\tau$ with increasing $Q^\perp$ in the transparent regime. Besides the acousto-optic resonance there occurs a resonance at the plasma edge ($\omega_i\tau\cong35.1$) independent of the acoustic frequency. This resonance is associated with the dramatic changes in the real and imaginary parts of the plasmariton dispersion relation around the plasma edge. Also, one should note the shoulder on the low-frequency side of the plasma edge resonance for $Q^\perp=2\times10^6$ m^{-1}. In Al this shoulder develops into a peak. A calculation of the scattering intensities based on the near-local approximation gives a result which deviates insignificantly from that shown in Fig. 13.

By increasing the acoustic wave vector 1 or 2 orders of magnitude the acousto-optic scattering can be tuned into resonance with the plasmonlike part of the electromagnetic field. This is illustrated in Fig. 14, where we have plotted the normalized scattering intensity $I^{p\to s}$ as a function of $\omega_i\tau$ for $Q^\perp=4\times10^7$ m^{-1} ($\Omega\cong92$ GHz) and $Q^\perp=8\times10^7$ m^{-1} ($\Omega\cong184$ GHz). For comparison is shown also the result of a near-local approximation, demonstrating the incorrect predictions of the scattering intensity provided by this model away from the plasma edge in the L-mode case. As in the preceding figure the acousto-optic resonances are displaced toward higher opti-

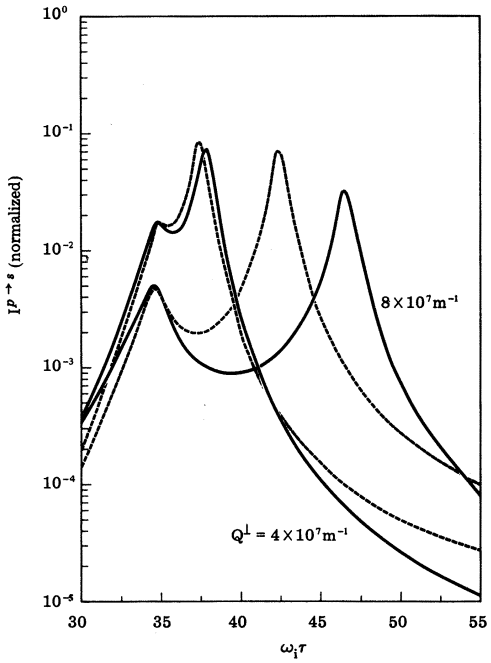

FIG. 14. Normalized anti-Stokes intensity $I^{p\to s}$ in n-type InSb for the p-s scattering configuration as a function of the dimensionless optical frequency $\omega_i\tau$ for two acoustic wave vectors $Q^\perp=4\times10^7$ m^{-1} and 8×10^7 m^{-1}. The optical and acoustic angles of the incidence are $\theta=5°$ and $\phi=0°$. The nonlocal and near-local calculations have been indicated by solid and broken curves, respectively. The resonances essentially stem from the interaction with the plasmonlike part of the incident field.

cal frequencies with increasing acoustic frequency in the transparent regime. Thus the resonances occur at $\omega_i\tau \cong 37.9$ and 46.5. The corresponding resonances in the near-local approximation are at $\omega_i\tau \cong 37.4$ and 42.4, respectively. Furthermore, note the plasma edge resonances.

Finally, let us turn our attention to Al. Thus in Fig. 15 is shown $I^{p\to s}$ as a function of $Q^{\perp}$ for three frequencies ($\omega_i\tau = 178$, 180, and 184) around the plasma edge. The calculations are based on the nonlocal approach but the near-local theory gives essentially the same results. Qualitatively, the curves are as those for n-type InSb showing characteristic T- and L-mode resonances at $Q^{\perp} \cong 3.25\times 10^7 \mathrm{m}^{-1}$ and $3.35\times 10^9 \mathrm{m}^{-1}$, respectively. However, one should note that the resonance with the plasmonlike part of the electromagnetic field occurs at an acoustic wave vector halfway out in the Brillouin zone. The scattering intensity has been normalized to unity at the T resonance shown in Fig. 16.

The scattering intensity taken as a function of the dimensionless optical frequency is shown for $Q^{\perp}=6\times 10^7$ m^{-1} ($\Omega \cong 193$ GHz) in Fig. 16 and for $Q^{\perp}=6\times 10^9$ m^{-1} (corresponding to a frequency a little bit less than that predicted on the basis of a dispersion-free phonon model, i.e., $\Omega \approx 1.93\times 10^4$ GHz) in Fig. 17. The resonance at $\omega_i\tau \cong 193.8$ in Fig. 16 stems from the plasmaritonlike part of the incident field, and that at $\omega_i\tau \cong 194.7$ (Fig. 17) from the plasmonlike part. As for n-type InSb resonances occur at the plasma edge, too. The near-local approach shifts the L-mode resonance to $\omega_i\tau \cong 192.3$.

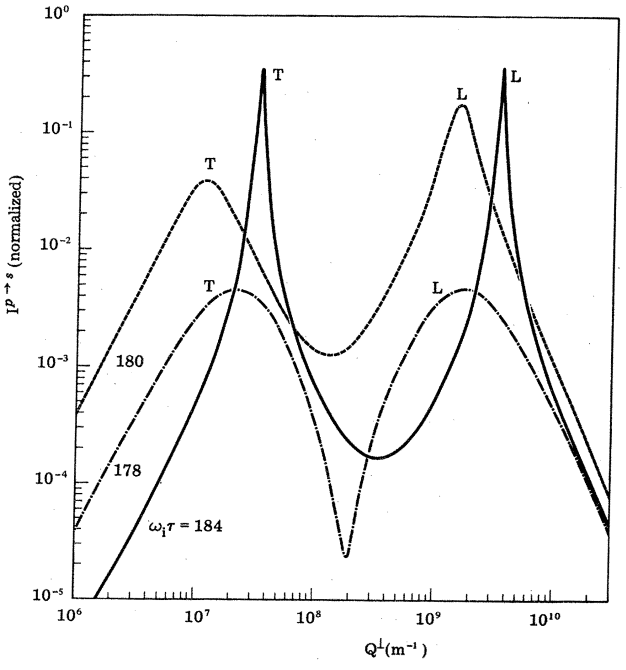

FIG. 15. Normalized anti-Stokes intensity $I^{p\to s}$ in Al for the p-s scattering configuration as a function of the acoustic wave vector $Q^{\perp}$ for three different dimensionless optical frequencies $\omega_i\tau = 178$, 180, and 184 around the plasma edge. The optical and acoustic angles of incidence are $\theta = 5°$ and $\phi = 0°$, respectively. The plasmaritonlike and plasmonlike resonances have been labeled by T and L, respectively. The nonlocal and near-local approaches give essentially the same result.

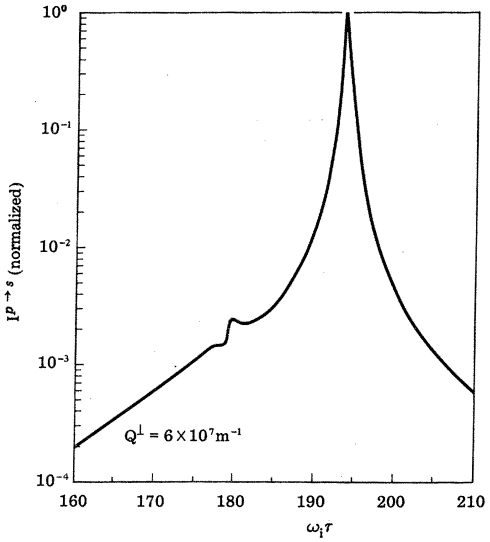

FIG. 16. Normalized anti-Stokes intensity $I^{p\to s}$ for the p-s scattering configuration as a function of the dimensionless optical frequency $\omega_i\tau$ for an acoustic wave vector $Q^{\perp}=6\times 10^7$ m^{-1}. The optical and acoustic angles of incidence are $\theta = 5°$ and $\phi = 0°$, respectively. The resonances essentially stem from interaction with the plasmaritonlike part of the incident field. Nonlocal and near-local approaches give the same result.

VI. CONCLUDING REMARKS

The theory of acousto-optic scattering of opaque media presented in this work has been established essentially by

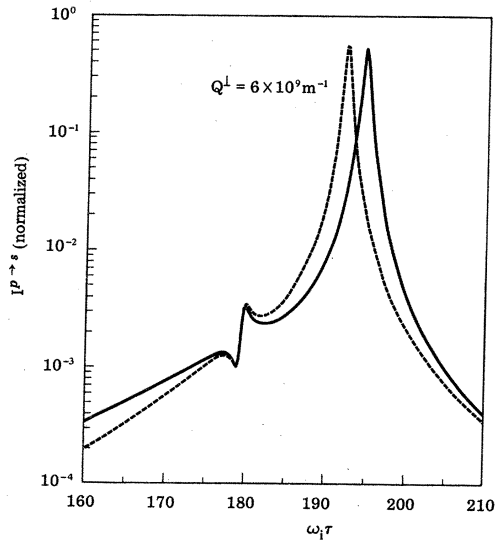

FIG. 17. Normalized anti-Stokes intensity $I^{p\to s}$ in Al for the p-s scattering configuration as a function of the dimensionless optical frequency $\omega_i\tau$ for an acoustic wave vector $Q^{\perp}=6\times 10^9$ m^{-1}. The optical and acoustic angles of incidence are $\theta = 5°$ and $\phi = 0°$, respectively. The nonlocal and near-local calculations have been indicated by solid and dashed curves, respectively. The resonances essentially stem from the interaction with the plasmonlike part of the incident field.

means of methods used in studies of the anomalous skin effect[47] and the photoemission process.[45] As mentioned in the Introduction these methods almost[6] seem to have been overlooked in light scattering investigations. Dresselhaus and Pine,[6,48] however, have made calculations of light scattering line shapes in opaque materials in the spirit of skin-effect studies. Their analyses are restricted to the case where the optical and acoustic waves are propagating perpendicular to the surface. Unfortunately, it turns out that the line shape they obtain differs from that obtained by Dervisch and Loudon,[7] who have used the mathematical devices which are conventional for light scattering studies. The disagreement can be traced back to the fact that Dresselhaus and Pine neglect the field derivative $\vec{g}$ of the anti-Stokes (or Stokes) field at the surface [compare Eq. (48) of Ref. 38 and Eq. (3.3) of this paper with the equations (unnumbered) for the Fourier components of the incident and scattered fields in the paper by Dresselhaus and Pine[6]]. By taking into account the appropriate field gradient at the surface we obtain for the scattered light intensity the result in Eq. (3.47). In the local limit, where the inelastic scattering from the plasmonlike part of the incident field vanishes, Eq. (3.47) exactly reduces, for perpendicular incidence of the light and sound waves, to the local result obtained by Loudon[7] [see Eq. (8) of Ref. 7].

The value of using the "skin-effect method" does not lie in the fact that this method gives the same result as the conventional one, but in the circumstance that *nonlocal* optical properties of the metal (or semiconductor) can be taken into account. Of these properties it has been demonstrated in the present paper that the branch-cut and the plasmon-like contributions are of significant importance.

The present work has been limited in several aspects. First of all, we have considered the scattering from a single acoustic mode only. To treat thermal Brillouin scattering one must consider the effect of superimposing the scattering from the thermal spectrum of surface and bulk waves, including for instance the scattering from the surface ripple mechanism. Secondly, the importance of the nonlocal optical properties of the metal (or semiconductor) not least in the opaque frequency regime shows that the properties of the electromagnetic field close to the surface are of significance. This implies that one must study the effect of replacing the sharp electron-density profile in the surface with a smooth one. At this stage in the development of the theory the Boltzmann-equation treatment must be abandoned, and a quantum theory, based on the density matrix formalism, which treats the nonlinear Brillouin-scattering response of an inhomogeneous jellium must be established.[49] Thirdly, the calculation of inelastic scattering cross sections is inseparably connected with a study of energy-transport velocities, a subject of importance in itself. Finally, dynamic inelastic scattering effects which cannot be treated within the framework of a parametric approximation, seem to be of importance in the opaque frequency regime.[28]

In this analysis it has been assumed that the scattering of the electrons from the surface is specular. For well-polished surfaces, it is known[33–36] from the linear optical properties of the metals, that the specular scattering model is in fair agreement with experimental observations. From a theoretical point of view the analytical treatment of diffuse scattering is much more involved than that presented here as it is demonstrated in Ref. 37. Furthermore, to develop nonlocal theories toward the description of smooth electron surface profiles, at the present state of the art, it seems most appropriate to take as a starting point the specular scattering model.

[1] J. R. Sandercock, Phys. Rev. Lett. 28, 237 (1972).
[2] J. R. Sandercock, Phys. Rev. Lett. 29, 1735 (1972).
[3] B. I. Bennett, A. A. Maradudin, and L. R. Swanson, Ann. Phys. (N.Y.) 71, 357 (1972).
[4] J. S. Nkoma and R. Loudon, J. Phys. C 8, 1950 (1975).
[5] D. L. Mills, Y. J. Chen, and E. Burstein, Phys. Rev. B 13, 4419 (1976).
[6] G. Dresselhaus and A. S. Pine, Solid State Commun. 16, 1001 (1975).
[7] A. Dervisch and R. Loudon, J. Phys. C 9, L669 (1976).
[8] S. Mishra and R. Bray, Phys. Rev. Lett. 39, 222 (1977).
[9] J. R. Sandercock, Solid State Commun. 26, 547 (1978).
[10] R. Loudon, Phys. Rev. Lett. 40, 581 (1978).
[11] A. Dervisch and R. Loudon, J. Phys. C 11, L291 (1978).
[12] N. L. Rowell and G. I. Stegeman, Solid State Commun. 26, 809 (1978).
[13] N. L. Rowell and G. I. Stegeman, Phys. Rev. B 18, 2598 (1978).
[14] B. Bortolani, F. Nizzoli, and G. Santoro, J. Phys. F 8, L215 (1978).
[15] J. G. Dil and E. M. Brody, Phys. Rev. B 14, 5218 (1976).
[16] R. Loudon, J. Phys. C 11, 403 (1978).
[17] R. Loudon, J. Phys. C 11, 2623 (1978).
[18] K. R. Subbaswamy and A. A. Maradudin, Ind. J. Pure Appl. Phys. 16, 282 (1978).
[19] K. R. Subbaswamy and A. A. Maradudin, Phys Rev. B 18, 4181 (1978).
[20] H. N. Spector, Solid State Phys. 19, 291 (1966).
[21] V. V. Proklov, G. N. Shkerdin, and Yu. V. Gulyaev, Solid State Commun. 10, 1145 (1972).
[22] O. Keller, in *Proceedings of the Third International Conference on Light Scattering in Solids,* edited by M. Balkanski, R. C. C. Leite, and S. P. S. Porto (Flammarion, Paris, 1976), p. 447.
[23] O. Keller, Phys. Rev. B 13, 4612 (1976).
[24] S. Fukuda, T. Karasaki, T. Shiosaki, and A. Kawabata, Phys. Rev. B 20, 4109 (1979).
[25] O. Keller, J. Opt. Soc. Am. 68, 42 (1978).
[26] G. Borrman, Z. Phys. 127, 297 (1950).
[27] B. W. Batterman and H. Cole, Rev. Mod. Phys. 36, 681 (1964).
[28] O. Keller, Phys. Rev. B 19, 2175 (1979).
[29] O. Keller, in *Proceedings of the Fourteenth International Conference on the Physics of Semiconductors,* edited by B. L. H. Wilson (IOP, London, 1979), p. 1363.
[30] O. Keller, Solid State Commun. 39, 1243 (1981).
[31] D. L. Mills and K. R. Subbaswamy, in *Progress in Optics,* edit-

ed by E. Wolf (North-Holland, Amsterdam, 1981), Vol. 11, p. 45.
[32]F. Forstman, Z. Phys. 203, 495 (1967).
[33]K. L. Kliewer and R. Fuchs, Phys. Rev. 172, 607 (1968).
[34]R. Fuchs and K. L. Kliewer, Phys. Rev. 185, 905 (1969).
[35]A. R. Melnyk and M. J. Harrison, Phys. Rev. B 2, 835 (1970).
[36]A. R. Melnyk and M. J. Harrison, Phys. Rev. B 2, 851 (1970).
[37]J. M. Keller, R. Fuchs, and K. L. Kliewer, Phys. Rev. B 12, 2012 (1975).
[38]O. Keller, Phys. Rev. A 26, 1742 (1982).
[39]O. Keller, J. Phys. C 15, 329 (1982).
[40]O. Keller, J. Opt. Soc. Am. 72, 1273 (1982).
[41]O. Keller (unpublished).
[42]D. F. Nelson, *Electric, Optic, and Acoustic Interactions in Dielectrics* (Wiley, New York, 1979).
[43]R. Claus, L. Merten, and J. Brandmüller, *Light Scattering by Phonon-Polaritons,* Vol. 75 of *Springer Tracts in Modern Physics* (Springer, Berlin, 1975), p. 176.
[44]J. Lindhard, K. Dan. Vidensk. Selsk. Mat.-Fys. Medd. 28, No. 8,1 (1954).
[45]F. Wooten, *Optical Properties of Solids* (Academic, New York, 1972).
[46]H. Kuzmany, Phys. Status Solidi A 25, 9 (1974).
[47]J. Callaway, *Quantum Theory of the Solid State* (Academic, New York, 1974), p. 619.
[48]A. S. Pine and G. Dresselhaus, in *Proceedings of the Third International Conference on Light Scattering in Solids,* edited by M. Balkanski, R. C. C. Leite, and S. P. S. Porto (Flammarion, Paris, 1976), p. 138.
[49]O. Keller (unpublished).